AFRL-AFOSR-UK-TR-2016-0001

Combining two-photon polymerisation and photoreduction to enable the manufacture of metamaterials at the nanoscale

Ricky Wildman
UNIVERSITY OF NOTTINGHAM

01/13/2016
Final Report

Air Force Research Laboratory
AF Office Of Scientific Research (AFOSR)/ IOE
Arlington, Virginia 22203
Air Force Materiel Command

REPORT DOCUMENTATION PAGE

Form Approved OMB No. 0704-0188

1. REPORT DATE ***(DD-MM-YYYY)*** 1 Sep 2015	**2. REPORT TYPE** Final Report	**3. DATES COVERED** *(From – To)* 15 Jan 2014 – 14 Jul 2015

4. TITLE AND SUBTITLE

Combining two-photon polymerisation and photoreduction to enable the manufacture of metamaterials at the nanoscale

5a. CONTRACT NUMBER
EOARD 14-0048

5b. GRANT NUMBER
FA9550-14-1-0048

5c. PROGRAM ELEMENT NUMBER
61102F

5d. PROJECT NUMBER

5d. TASK NUMBER

5e. WORK UNIT NUMBER

6. AUTHOR(S)

Qin Hu, Yaan Liu, Ricky Wildman, Christopher Tuck and Richard Hague

7. PERFORMING ORGANIZATION NAME(S) AND ADDRESS(ES)
UNIVERSITY OF NOTTINGHAM
UNIVERSITY PK
NOTTINGHAM NG72RD UNITED
KINGDOM

8. PERFORMING ORGANIZATION REPORT NUMBER
N/A

9. SPONSORING/MONITORING AGENCY NAME(S) AND ADDRESS(ES)

EOARD
Unit 4515
APO AE 09421-4515

10. SPONSOR/MONITOR'S ACRONYM(S)
AFRL/AFOSR/IOE (EOARD)

11. SPONSOR/MONITOR'S REPORT NUMBER(S)

12. DISTRIBUTION/AVAILABILITY STATEMENT

Distribution A: Approved for public release; distribution is unlimited.

13. SUPPLEMENTARY NOTES

14. ABSTRACT

In this project, we investigated the feasibility of a new method of manufacturing metamaterials by combining two-photon polymerisation (2PP) and photoreduction. A new rig has been built for this purpose. The polymerisation of four materials, OrmoComp, SU8, IPL and PEGDA, based on different polymerisation mechanisms, has each been investigated. Au salt photoreduction has been demonstrated. Polymer-metal hybrid two-photon processing has been tested by mixing each of the four polymers with Au salt. The formulations for simultaneous polymerisation and reduction have been optimised, and methods for controlling each process independently have been explored. The use of a 532 nm laser in addition to the near IR laser for two photon absorption, has afforded control over the degree of polymerisation and reduction evident during fabrication.

15. SUBJECT TERMS

EOARD, Materials, nano-scale manufacturing

16. SECURITY CLASSIFICATION OF:			**17. LIMITATION OF ABSTRACT**	**18, NUMBER OF PAGES**	**19a. NAME OF RESPONSIBLE PERSON** Matthew Snyder
a. REPORT UNCLAS	**b. ABSTRACT** UNCLAS	**c. THIS PAGE** UNCLAS	SAR	40	**19b. TELEPHONE NUMBER** *(Include area code)* +44 (0)1895 616420

Standard Form 298 (Rev. 8/98)
Prescribed by ANSI Std. Z39-18

Combining two-photon polymerisation and photoreduction to enable the manufacture of metamaterials at the nanoscale

September 2015

Qin Hu, Yaan Liu, Ricky Wildman, Christopher Tuck and Richard Hague

Additive Manufacturing and 3D Printing Research Group

Executive Summary

In this project, we investigated the feasibility of a new method of manufacturing metamaterials by combining two-photon polymerisation (2PP) and photoreduction. A new rig has been built for this purpose. The polymerisation of four materials, OrmoComp, SU8, IPL and PEGDA, based on different polymerisation mechanisms, has each been investigated. Au salt photoreduction has been demonstrated. Polymer-metal hybrid two-photon processing has been tested by mixing each of the four polymers with Au salt. The formulations for simultaneous polymerisation and reduction have been optimised, and methods for controlling each process independently have been explored. The use of a 532 nm laser in addition to the near IR laser for two photon absorption, has afforded control over the degree of polymerisation and reduction evident during fabrication.

Table of contents

1. Introduction

The techniques currently available for fabrication at the nanoscale are mainly based on traditional microchip patterning techniques, e.g. photolithography combined with metal deposition, which are expensive, multistep and slow, often prone to failure and material waste and to date with insufficient control to truly form multimaterial components. Multiphoton absorption and subsequent photochemistry offers a route to avoiding the drawbacks of lithography, whilst also enabling 3D manufacture at a sub-micron length scale. Not only does it allow polymerisation, it enables photoreduction and raises the possibility of combining these two processes for multimaterial fabrication. In this project, we investigate the feasibility of combining two-photon polymerisation (2PP) and photoreduction in a selective and controlled manner to afford multimaterial fabrication on the nanoscale.

1.1. Two-photon polymerisation

Two-photon polymerisation works by scanning a femto-second laser through a 3D space. A photosensitizer absorbs two photons within a short period of time to jump from the ground state to the excited state, and then pass its energy to photoinitiator to create an active centre and on to chain-growth polymerisation. Non-linear two photon absorption (2PA) means that high resolution can be achieved allowing complex 3D structures to be fabricated with feature sizes of the order of 10s of nm. Polymerization only occurs where the intensity of a laser pulse is over the threshold required to initiate electron promotion and since this occurs only in a narrow band within the laser beam profile, feature sizes can be below the diffraction limit of light. The mechanism of two-photon polymerisation is illustrated in Figure 1-1.

Compared to other manufacturing techniques, two-photon polymerisation has the following advantages:

- Fabricate complex true-3D micro/nano structures
- Direct fabrication without a mask
- Sub-100-nm feature size is achievable
- A variety of materials can be processed
- Cost-effective: no vacuum or clean-room is required

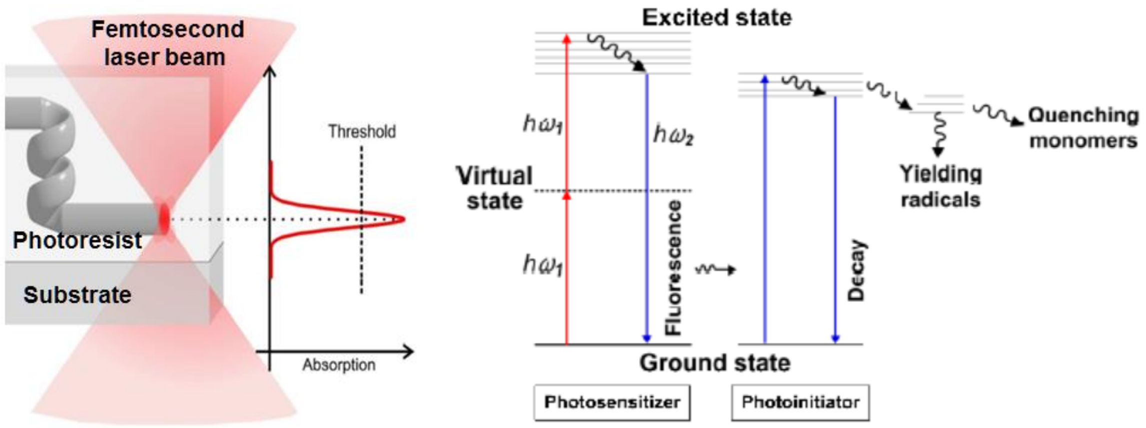

(a) (b)

Figure 1-1: (a) Illustration of two-photon polymerisation. (b) Schematic energy level diagram of two-photon polymerisation. Image from ref. (Jung, Kong et al. 2011).

1.2. Two-photon reduction

As 2PA is highly localised at the focus to a volume of order of λ^3 (where λ is the laser wavelength), it is possible to confine successive chemical or physical reactions also in this small volume. By utilizing this unique property of the 2PA, metallic micro/nanostructures can be fabricated by two-photon induced reduction of metal complex ions, which normally involves stages such as nanoparticle nucleation, growth and aggregation, as illustrated in Figure 1-2.

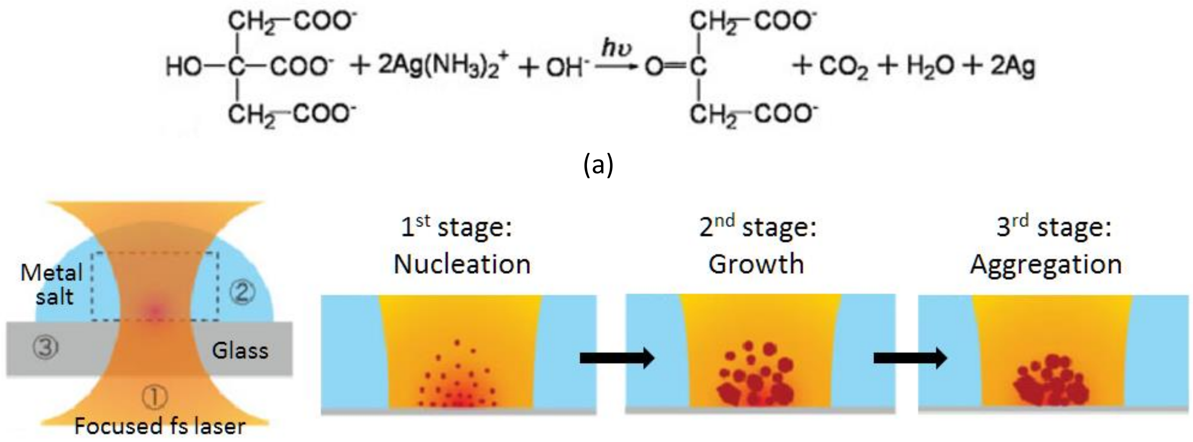

$$\mathrm{HO-\underset{CH_2-COO^-}{\overset{CH_2-COO^-}{C}}-COO^-} + \mathrm{2Ag(NH_3)_2^+} + \mathrm{OH^-} \xrightarrow{h\upsilon} \mathrm{O{=}\underset{CH_2-COO^-}{\overset{CH_2-COO^-}{C}}} + \mathrm{CO_2} + \mathrm{H_2O} + \mathrm{2Ag}$$

(a)

(b)

Figure 1-2: (a) Proposed equation for silver nitrate reduction in a mixture with ammonia and trisodium citrate (Xu, Xia et al. 2010). (b) Illustration of metal formation through two-photon reduction. Image was modified from ref. (Cao, Takeyasu et al. 2009).

1.3. Combining two-photon polymerisation and reduction

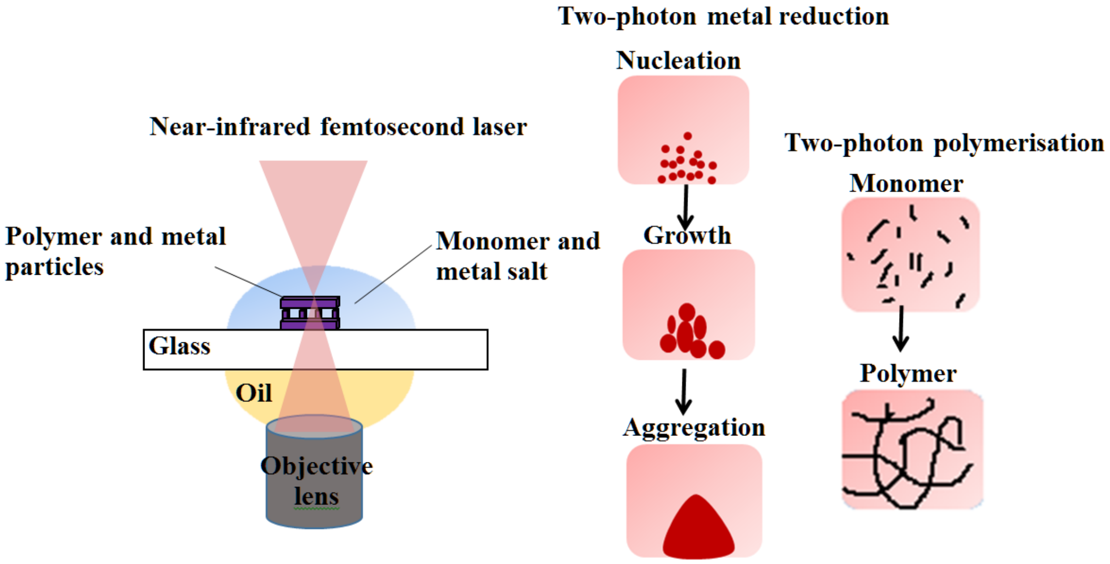

Figure 1-3: Illustration of fabricating nano-composites in a single step by two-photon induced polymerisation and metal salt reduction

Fabricating nano-composites in a single step by two-photon induced polymerisation and metal salt reduction is illustrated in Figure 1-3. A near-infrared femtosecond laser beam is focused into a photo-reactive resin containing a mixture of monomer and metal salt. A photoinitiator is excited by the simultaneous absorption of two photons, which can trigger local chemical reactions, including monomer cross linking and metal salt reduction. In this way, both polymer and metal nanoparticles can be formed. Due to high surface tension, the generated metal nanoparticles tend to aggregate into large ones. The local monomer cross linking may serve as a matrix, thus reducing the diffusion-related metal aggregation. These two simultaneous chemical reactions may compete with each other, leading to different morphology.

Figure 1-4 shows a schematic that summarises the main chemical steps that proceed during two-photon activation. Usually, a photopolymerisation (or reduction) process relies on the absorption of a single photon of sufficient energy to promote an electron either out of the upper most energy level if one wishes to produce radicals, or to an upper level prior to fluorescence and a secondary stage of reaction. The basis of two photon absorption is that two photons of a lower energy than that in the single absorption process are absorbed simultaneously, the combination of which is sufficient to promote the electron. Because of the lower probability of simultaneous absorption and the consequent narrower absorption cross-section, a higher spatial resolution is achieved, typically for two-photon polymerisation reactions structures of the order 100nm are produced. In order to initiate sufficient events, a high intensity femto-second pulse laser is required. The principle that we wish to exploit is that this two-photon absorption can be used for both polymerisation and for photo-reduction. The former can be used to generate a polymeric matrix or substrate, whilst the latter can be used for the creation of metallic structures or nanoparticle production. Appropriate selection of the materials and the wavelength of the beam mean that one has control over one of the processes – the lower energy process – by tuning the wavelength of the incident light. That is, we can choose the two-photon energy level to be such that it will drive one process, but be insufficient to drive the other. However, if we wish to drive the higher energy process, it is inevitable that will initiate both polymerisation and photoreduction and there is no separate control.

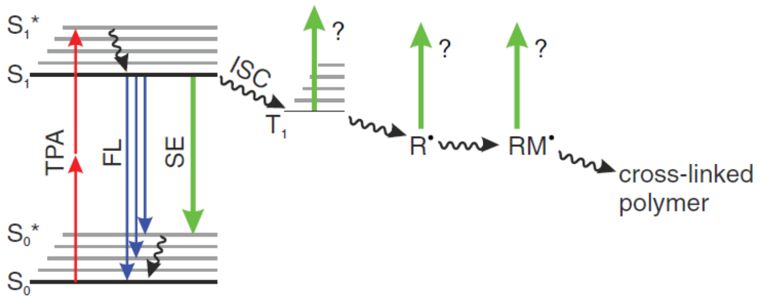

Figure 1-4: Schematic diagram showing the relevant molecular transitions and subsequent transient states. Two-photon absorption (TPA), fluorescence (FL), stimulated emission (SE), inter-system crossing (ISC), singlet states (Sx), triplet state (T1), initiating radical (R*), propagating polymer chain (RM*). Image from ref. (Fischer and Wegener 2012).

A solution to this is to employ the concept of stimulated emission depletion (STED), which was first proposed by Prof Stefan Hell who won Nobel Prize in Chemistry in 2014 for his contribution to the STED-based super-resolution microscopy. Photoreduction is a complex process usually consisting of several short-lived metastable reaction states. If we were to retard an early stage of this process we would be able to avoid the photo-reduction completely. It has been observed that the first step is a fluorescence mode where an electron is promoted to a higher energy state, which is followed by a cascade down the energy levels. Stimulated emission of photons between the lowest promoted energy state and the initial state will deplete the upper energy bands completely, bringing the reaction to a halt.

Complete control over polymerisation and photoreduction will then be afforded by two lasers, operating at different frequencies, driving either (i) 2PR or (ii) 2PP+2PR. Selective 2PP will then be enabled in step ii) by employing STED retarding 2PR and resulting in 2PP only.

1.4. Photoinitiators

The materials used for two-photon processing not only include the main monomer, e.g., SU8 and IPL, but also include suitable photosensitizer, photoinitiator and maybe surfactant (NOTE: Many additions have the function of both sensitizer and initiator, and they are often simply called initiator). Although these additions only take a small amount, normally less than 5 wt% of the mixture, they play a key role in two-photon induced reactions. Commercial resists, such as SU8, are designed for traditional photolithographic application by UV curing, and the initiators inside are not optimised for 2PA and normally exhibit low photosensitivity as the initiators tend to have small 2PA cross-sections, thus long exposure times and a high laser power is required for two-photon excitation (Cumpston, Ananthavel et al. 1999; Zhou, Kuebler et al. 2002; Pawlicki, Collins et al. 2009). Improvements in fabrication are therefore possible by combining a sensitizer with a large 2PA cross-section with an initiator with high quantum efficiency (Cumpston, Ananthavel et al. 1999; Li, Pucher et al. 2013). The laser energy needed for polymerisation and reduction can also be adjusted by sensitizers and initiators (Li, Pucher et al. 2013). This is crucial for selective control of the two processes at the same time. The desired two-photon sensitizers and initiators should have (a) a chromophoric group with a large cross-section, such as motifs D-π-D, D-π-A-π-D and A-π-D-π-A (where π is a π-conjugated bridge, D is a donor and A is an acceptor); (b) a functionality to generate the initiating species with high efficiency, such as those used in UV initiators; and (c) a mechanism through which excitation of the chromophore leads to activation of the chemical functionality, such as an electron transfer process (Cumpston, Ananthavel et al. 1999; Zhou, Kuebler et al. 2002; Li, Pucher et al. 2013).

1.5. Project management

To meet our aim of proof of concept for single step manufacture of hybrid metamaterials by combining two-photon polymerisation and photoreduction, we split the investigation into 3 work-packages (WP) each with its own associated objectives and deliverables. Work-package 3 has been modified with additional objectives and deliverables attributed to the extension:

WP1	**Material selection & system setup**
Objectives	O1 – Identification of suitable starting materials and combinations for two photon polymerisation and two photon metal reduction and complete optical system setup
Description: Suitable polymer resins and metallic salts/acids and their combinations will be identified. Optical system for two-photon process will be designed & built.	
Duration & Resource	2 Months PDRA
Deliverables	D1.1 – Suitable testing materials D1.2 – Two-photon operating system

WP2	**Single material two-photon processing**
Objectives	O2 – To demonstrate two photon polymerisation in isolation O3 – To demonstrate two photon driven metal reduction in isolation
Description: WP2 will investigate single-material structures fabricated by two-photon induced polymerisation and metal reduction, and identify the suitable parameter settings	

Duration & Resource	3 Months PDRA
Deliverables	D2.1 – Demonstrator of polymeric structures D2.2 – Demonstrator of metallic structures

WP3	**Two materials two-photon simultaneous processing**
Objectives	O4 – To demonstrate combined two photon polymerisation and photoreduction in a single process O5 – To demonstrate controlled and selective two photon polymerisation and photoreduction in a single process O6 – Reconfiguration of the rig to a "*bottom-up*" arrangement O7 – To demonstrate controlled and distributed nanoparticle arrays in polymeric matrices as a potential metamaterial O8 – To identify the future applications
Description: WP3 will reconfigure the 2PP set up to allow greater flexibility and stability and then go on to test its capability in the field of the manufacture of polymer-metal hybrid structures, and stimulated emission depletion in controlling the two simultaneous processes	
Duration & Resource	10 Months PDRA (including the 6-month extension)
Deliverables	Project Deliverable: D3.1 – Demonstration of controlled selective and distributed 3D two photon polymerisation and photoreduction in a single process D3.2 – A report summarising the capability, limitation and future work D3.3 – Journal publication

The three work packages are executed according the following workplan:

WP	**Description**	**Month** 1	2	3	4	5	6	7	8	9	10	11	12	13	14	15	**Deliverable**
1	Material selection	■															D1.1 – Suitable testing materials
	Optical system design & setup	■	■	■													D1.2 – Two-photon operating system
2	Polymer processing			■	■												D2.1 – Demonstrator of polymeric structures
	Metal processing			■	■	■											D2.2 – Demonstrator of metallic structures
3	Rig reconfiguration						■	■									D3.1 – Demonstration of controlled and selective processing
	Combined in a single process								■	■							
	Controlled and selective in a single process										■	■					
	Nanoparticle arrays in polymeric												■	■	■		

	matrices												▨	▨	▨		
	Identify future applications															■	D3.2 – Final report D3.3 – Publications

2. Experimental details

2.1. Laser-optical system

The nonlinear signal generating property of two-photon process requires high densities of excited photons. In order to accomplish this while at the same time maintaining relatively low average power on the sample, a femtosecond laser is preferred as the beam source. A modelocked Ti:Sapphire Chameleon Ultra I laser from Coherent is used in our lab. This laser has a tunable wavelength from 690 nm to 1040 nm. In the current study the wavelength is fixed at 780 nm. The pulse width of this laser is 140 fs and the repetition rate is 80 MHz. Laser power for polymerization ranges from sub-mW to hundreds of mW, depending on the material properties. In the current study the laser power is normally in the range of 20 mW to 75 mW. The laser beam is conditioned through a series of optics, e.g. a λ/2 wave plate, polarizer and beam expander, before it is divided into an objective lens for focus. An Olympus plan fluorite oil-immersion objective lens (100X, NA 1.3) is used. 3D fabrication is achieved through fixing the position of laser beam while moving the sample stage in X, Y and Z directions. The piezoelectric stage used in current study can travel 400 µm x 400 µm x 300 µm in X, Y and Z directions respectively, with resolution of 1 nm and repeatability of 10 nm. Our home-built setup for two-photon polymerisation is shown in Figure 2-1. The work shown in Section 5 used a commercial two-photon lithography system, Nanoscribe, benefitting from their software development for fabrication of complex 3D structures.

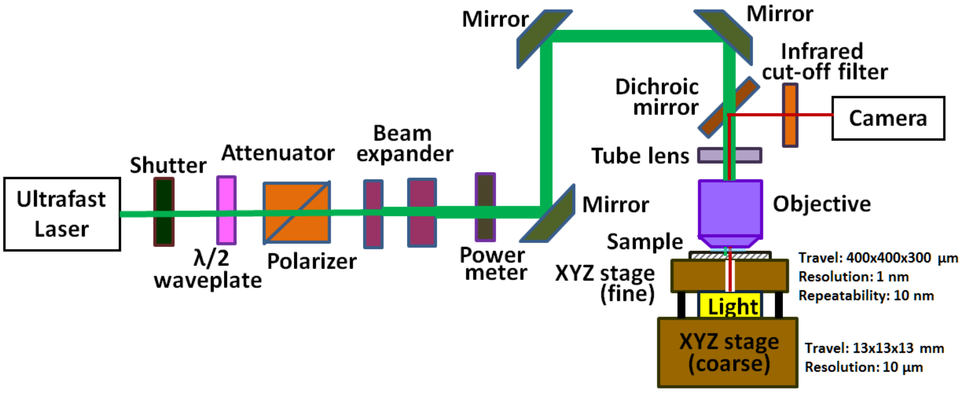

(a)

(b)

Figure 2-1: (a) Schematic diagram of two-photon polymerisation setup; (b) Picture showing Dr Qin Hu operating the two-photon polymerisation system to fabricate 3D micro/nano structures.

Two commonly used exposure strategies are shown in Figure 2-2. In the strategy shown in Figure 2-2(a), a sandwiched reservoir is made by two glass plates separated by a spacer. Fabrication starts from the top of the bottom glass plate and layer by layer builds up towards the objective lens. A standard 170 µm thick cover glass is used as the top glass plate. Due to the limitation of the working distance of high magnification lens, which is 200 µm for our case, and the thickness of immersion oil, structures with a maximum height of around 170 µm can be built in this exposure strategy. The bottom substrate can also be metal, silicon or other materials. In the second exposure strategy, which is shown in Figure 2-2(b), the glass plate which separates the immersion oil and the polymer resin also serve as the substrate, so the substrate is limited to a standard 170 µm thick cover glass. Due to the high viscosity of polymer resin, no sandwich configuration is needed. As the structure is built layer by layer away from the lens, the laser beam needs to pass through an already built structure, which may lead to some distortion and results in slight resolution or accuracy problems. Both exposure strategies have been used in the current study.

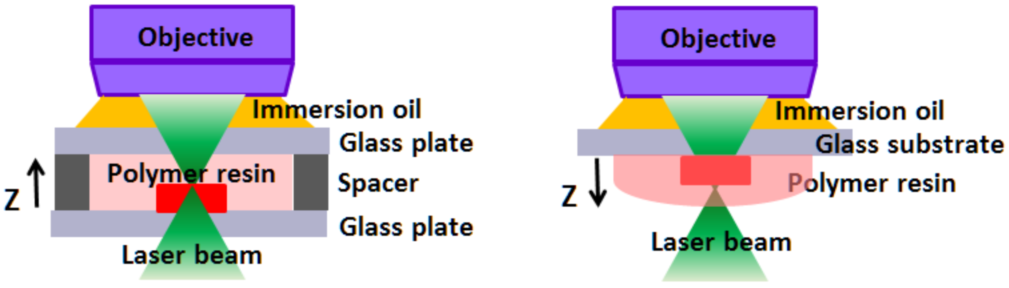

(a) (b)

Figure 2-2: Two different exposure strategies: (a) Polymer resin is placed inside a sandwiched reservoir made by two glass plates and spaces, and structure is built from the top of the bottom plates towards the objective lens; (b) the glass plate which separates the immersion oil and the polymer resin also serves as the substrate and structure is built from the bottom of the glass plate away from the objective lens.

The laser beam path in the '*top-down*' configuration (*objective lens on top of substrate*) shown in Figure 2-1 is prone to be affected by the environment, e.g., shaking, and thus may lead to the illumination being out of focus. Before the second laser is integrated into the two-photon polymerisation rig to incorporate STED functionality, it was decided that it was necessary to change the configuration into a '*bottom-up*' style, so the objective lens is placed under the substrate. In this way, the total length of the beam path was shortened and being closer to the optical table, external shaking induced out of focus can be reduced. The new rig including the two lasers is illustrated in Figure 2-3. The second laser is a Spectra-Physics Excelsior compact 532 nm 50 mW continuous wave (CW) solid state laser.

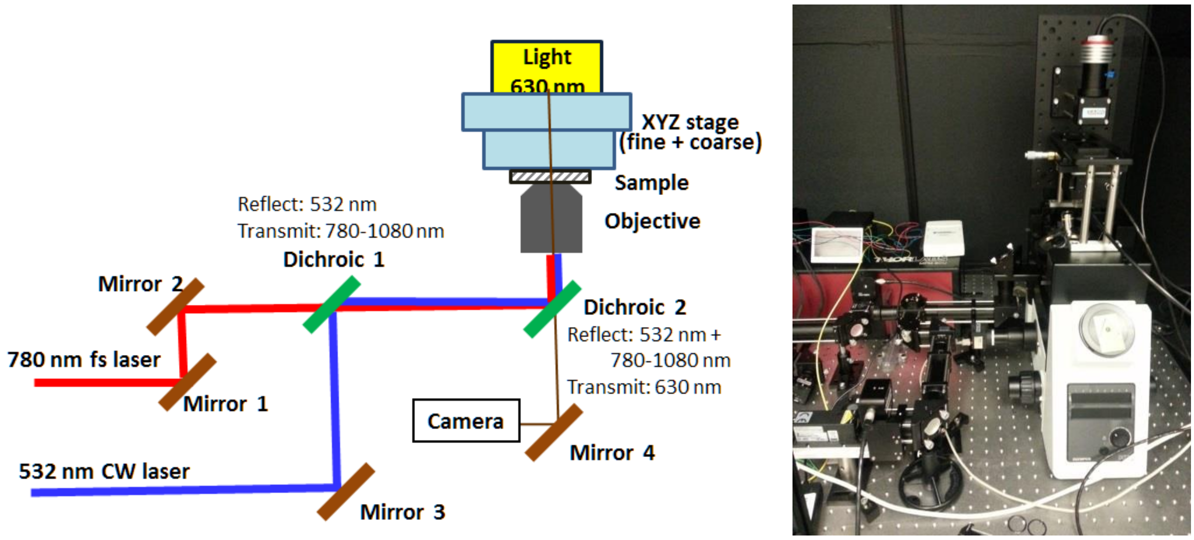

(a) (b)

Figure 2-3: (a) Schematic diagram of '*bottom-up*' setup for the rig including 780 nm femtosecond laser and 532 nm CW laser; (b) Picture showing the two-laser rig.

2.2. Fabrication procedures

The fabrication procedure is illustrated in Figure 2-4. The glass substrate needs to be cleaned before loading of the photoresist. Glass can be washed in acetone, isopropanol and water in sequence, then blow dried with nitrogen gas. Before laser processing, some photoresist may need pre-exposure treatment. For example, a glass substrate with OrmoComp needs to be held on a hotplate at 80^{o}C for 2 min to increase the resist homogeneity and the adhesion to the substrate. SU8 needs a prebake at 65^{o}C for 5 min followed with a softbake at 95^{o}C for 15 min. To build a structure from the substrate, the interface between the substrate and the resist needs to be found before laser exposure. This is particularly important for photoreduction. If metal nanoparticles are not fixed on to the substrate, they are washed away during the subsequent developing procedures. After 3D scanning with the laser to form the desired micro/nano structure, the unsolidified resist is washed away by rinsing using a solvent – developer. Before developing, some samples may also need postbake to increase the adhesion to the substrate. OrmoComp sample should be on hotplate at 130^{o}C for 10 min. After developing, some samples may also need hardbake to increase the thermal and environmental stability. OrmoComp structures should be baked at 150^{o}C for 3 hours. The polymer resist IPL developed by Nanoscribe does not need any heat treatment before and after laser exposure.

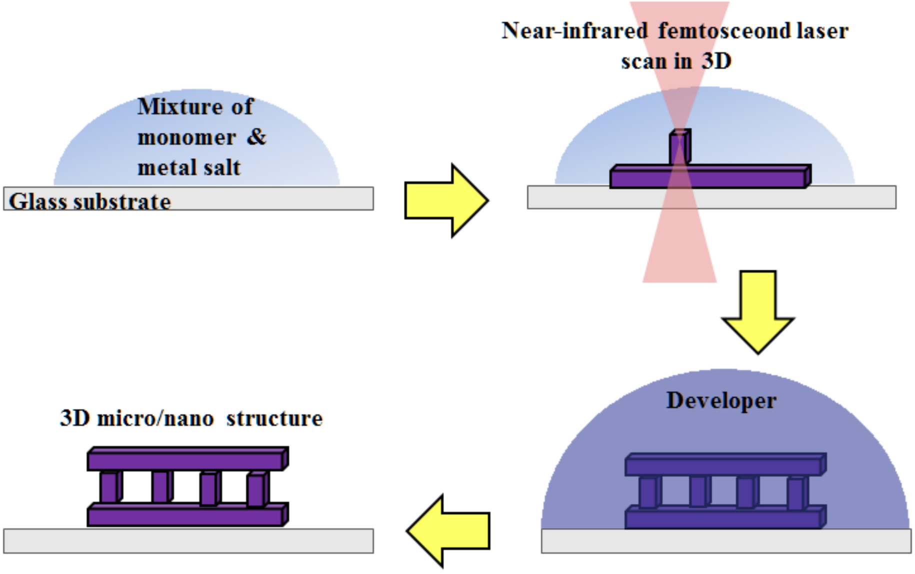

Figure 2-4: Schematic illustration of fabrication procedures

3. Two-photon polymerisation

3.1. Material selection

The material used for two-photon polymerisation needs to meet the following requirements (Wu, Serbin et al. 2006):

- Transparent in the near infrared region
- Fast curing speed so that only the material in the focal point is polymerized
- Resistant to the solvent used in the later washout process
- Suitable mechanical property and thermal stability to maintain shape

Two-photon polymerisation is chain-growth polymerisation initiated by the absorption of two photons. The mechanism can be grouped into radical-based polymerisation (*by which a polymer forms by the successive addition of free radical building blocks*) and ionic-based polymerisation (*by which the propagating species is a long chain cation or anion*), e.g., the acid-catalysed cationic polymerisation of epoxides. Ionic-based polymerisation is often preferred to radical polymerisation as the latter can lead to controlled diffusion lowering the spatial resolution and also is susceptible to oxygen quenching (Pawlicki, Collins et al. 2009). In the current study, four materials have been selected and include both polymerisation mechanisms. They are summarized in Table 3-1.

Depending on the used material and the configuration of each structure to be fabricated, the processing parameter settings are changed accordingly. The laser power is generally in the range of 20 mW to 75 mW. A higher laser power generates a bigger voxel of material and thus the feature size of the formed structure is bigger.

Both hard substrate (cover glass) and flexible substrate (polyester film) have been tested in the current study.

Table 3-1: Materials selected for two-photon polymerisation

	OrmoComp	**IPL**	**SU8**	**PEGDA**[*]
Mechanism for polymerisation	Radical + ionic	Unknown[**]	Ionic	Radical
Commercial or home developed	Commercial product for UV curing	Commercial product for two-photon polymerisation	Commercial product for UV curing	Home developed
Property after polymerisation	Solid	Solid	Solid	Hydrogel
Biocompatible?	Yes	No	Yes	Yes

[*] PEGDA is the short name for polyethylene (glycol) diacrylate.

[**] Supplier refused to provide its chemical composition, so the mechanism of polymerisation is not clear.

3.2. OrmoComp

Ormocer was first developed by the Fraunhofer Institut für Silicatforschung as an abbreviation for ORganically MOdified CERamics. It is a type of photosensitive inorganic-organic hybrid polymer, with combined properties of glasses and ceramics, organic polymers and silicones (see Figure 3-1). Its properties can be tailored according to the requirements for the application. Figure 3-2 shows the multifunctional precursors that are used for material synthesis and their effect on material properties.

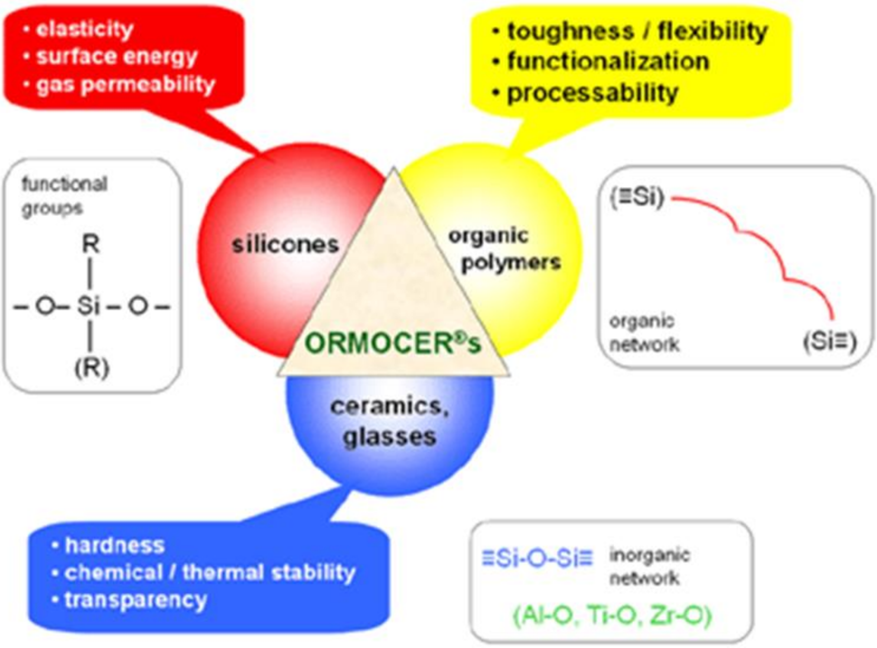

Figure 3-1: Schematic diagram showing the properties of Ormocer. Image from www.ormocer.de.

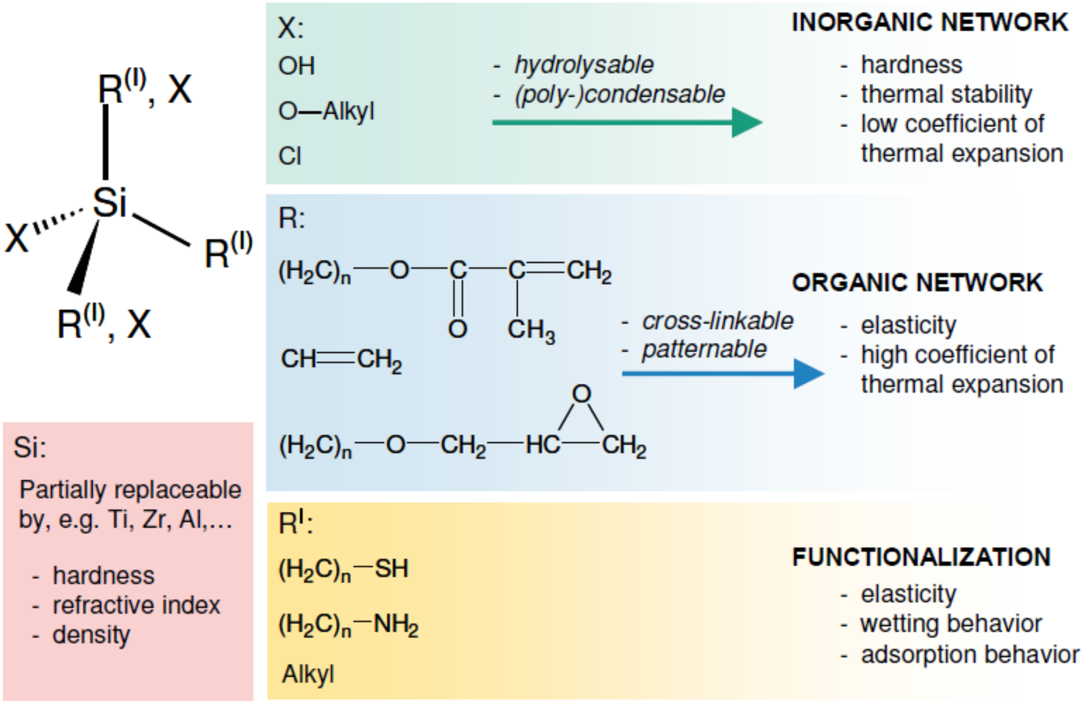

Figure 3-2: Multifunctional precursors for Ormocer synthesis and their contribution on material properties. Image from ref. (Houbertz, Steenhusen et al. 2010).

Ormocer has excellent physical, chemical, mechanical and optical properties. It remains stable up to 350^{o}C in an Oxygen rich environment and 415^{o}C in a Nitrogen environment. Ormocer's density (1.1~1.6 g/cm^{3}), Young's modulus (11-17,000 MPa), thermal expansion coefficient, gas permeability, refractive index (n = 1.47~1.56) and other properties are between those of ceramics and polymers. Parts of its mechanical properties are summarized in Table 3-2. It has a high flexural strength and high adhesive strength compared to many substrate materials such as polymers, glass and silicon wafers. Ormocer exhibits a much lower volume of shrinkage (~ 2%) compared to many sol-gel prepared materials that show over 20% volume shrinkage. This is due to its stable inorganic Si-O-Si network and the inclusion of fillers. Ormocer is optically transparent over the 400-1600 nm wavelength. It also has low optical loss in the near infrared range (< 0.06 dB/cm at 830 nm, < 0.6 dB/cm at 1550 nm). In addition, Ormocer is biocompatible. Due to its unique flexible properties, it has been widely used in many different areas, such as optics, microelectronics and biomedical devices.

Table 3-2: Mechanical properties of Ormocer (Manhart, Kunzelmann et al. 2000)

	Mean value (standard deviations)
Flexural strength [MPa]	103.0 (19.9)
Flexural modulus [GPa]	6.3 (0.9)
Fracture toughness KIC [MNm$^{-3/2}$]	1.6 (0.3)
Vickers hardness [HV 0.2/40]	65.8 (1.6)
Mean wear rate [µm^{3}/cycle]	2763

OrmoComp is a commercial hybrid photoresist in the Ormocer series. It is sourced from Microresist Int. Although OrmoComp is designed for UV curing, polymerisation at 780 nm can still start, propagate and terminate. The wavelength of 780 nm is nearly double the wavelength of its peak absorption in UV range. By absorbing two photons, the energy released is enough to initiate polymerisation. Thus no chemical modification, e.g., adding additional photoinitiator or senisitizer, is needed for OrmoComp to polymerise by the two-photon process. Figure 3-3 shows a pattern after two-photon polymerisation (a) before developing and (b) after developing. The laser power was 48 mW and the piezo stage scan speed was 10 µm/s. More 3D patterns fabricated by OrmoComp are shown in Figure 3-4.

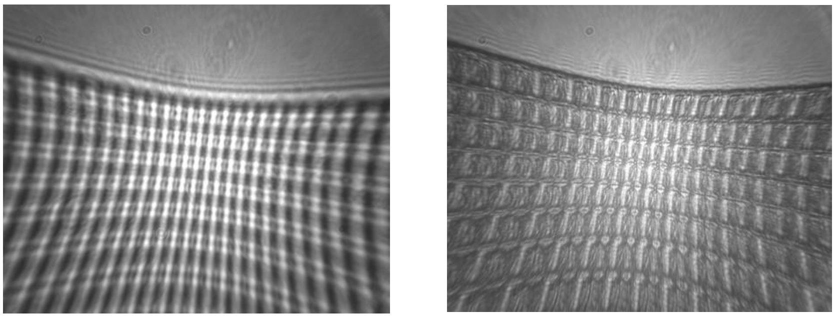

(a) (b)

Figure 3-3: Optical microscope image of OrmoComp (a) directly after laser processing but before developing, and (b) after developing.

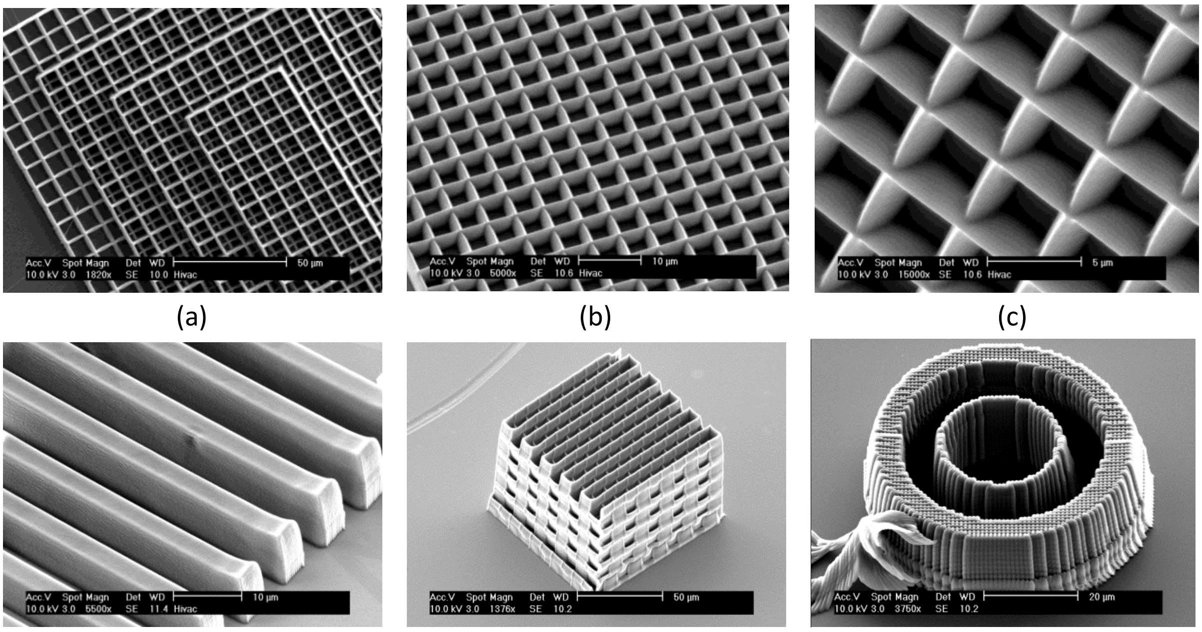

(a) (b) (c)

(d) (e) (f)

Figure 3-4: SEM images of various 3D micro/nano structures fabricated by OrmoComp two-photon polymerisation.

3.3. IPL

IPL is a commercial photoresist designed for two-photon polymerisation by Nanoscribe. The feature size of the structure made by IPL can reach 150 nm, the smallest among the all available photoresists. It has little shrinkage and good adhesion on glass substrates. Importantly, no prebake or postbake is needed. However, no chemical detail about this resist is available. Figure 3-5 shows some SEM images of micro/nano structures fabricated using IPL.

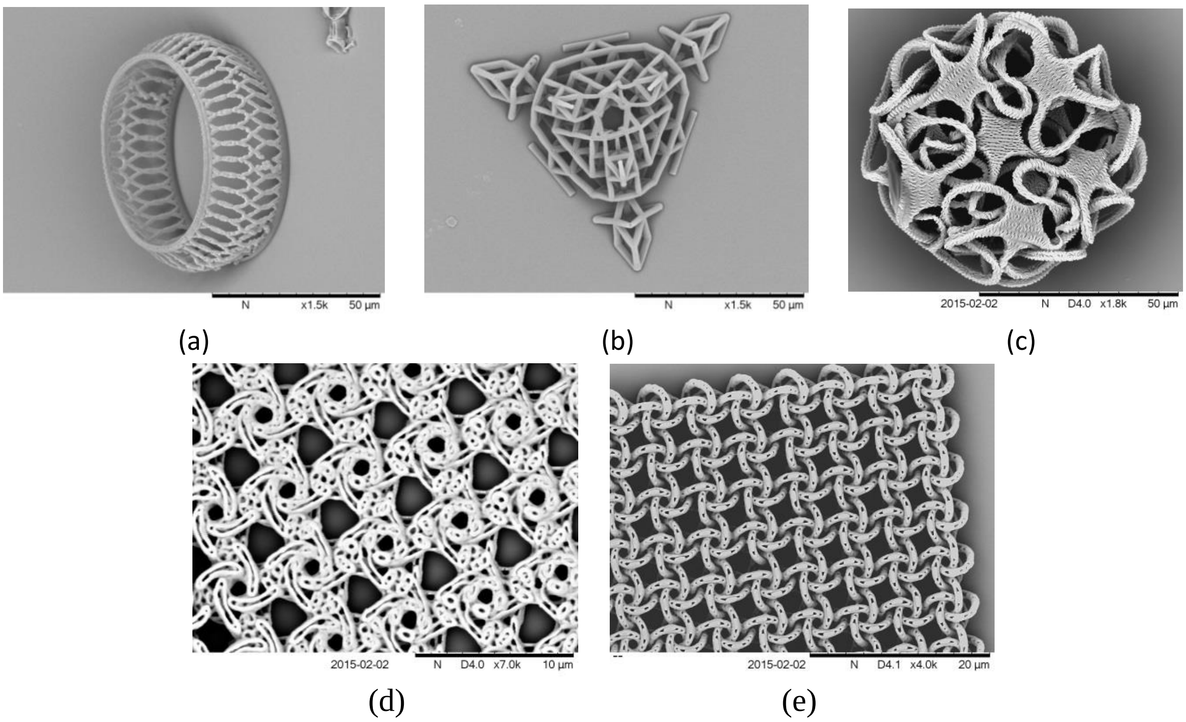

Figure 3-5: SEM images 3D micro/nano structures fabricated by two-photon polymerisation using IPL photoresist.

3.4. SU8

SU8 is a commonly used epoxy-based photoresist. Its chemical structure is shown in Figure 3-6. The resist used in the current study is sourced from Microchem with the photoacid generator PC2506, a diaryliodonium salt photoacid generator, $Ar_2I^+SbF_6^-$. Similar to OrmoComp, no chemical modification is needed for UV-curable SU8 to polymerise by the two-photon process at 780 nm. Its mechanical property after UV curing is shown in Table 3-3.

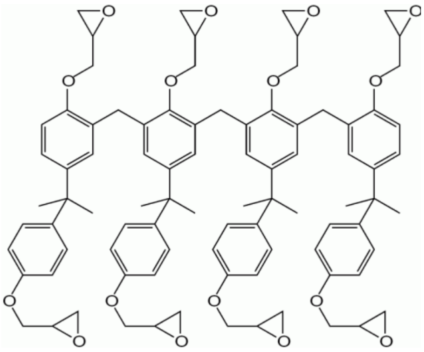

Figure 3-6: Chemical structure of SU8.

Table 3-3: Mechanical properties of SU8. Data are copied from the website http://www.microchem.com/pdf/SU8-table-of-properties.pdf

Property	**SU8 3000**
Softening point, DMA (°C)	200
Thermal Stability in Nitrogen, onset/5% weight loss (°C)	277/357
Thermal Stability in Air, onset/5% weight loss (°C)	
Young's Modulus (GPa)	2.0
Coeff. of Thermal Expansion, CTE (ppm/°C)	52
Tensile Strength (MPa)	73
Elongation at Break (%)	4.8
Thermal Conductivity (W/m°K)	0.2

3.5. PEGDA

PEGDA is a synthetic, hydrophilic starting material for hydrogel, with its structure unit shown in Figure 3-7. Its stiffness can be modulated from 10-100 kPa. It can have high water content and be customized to include a variety of biological molecules. It has been popularly used in cell culture and tissue engineering. PEGDA 250, photoinitiator DETX (2,4-Diethyl-9H-thioxanthen-9-one, 98%) and accelerator EDB (Ethyl 4-(dimethylamino)benzoate, 99wt%) are all bought from Sigma-Aldrich. They are mixed by weight ratio of 94:3:3 at room temperature in an amber vial, then stirred at 80°C for 3 mins until all the solutes were fully dissolved. Before laser processing, the mixture is degassed to remove dissolved oxygen, which can help to minimize any inhibition brought on by Oxygen. Laser power used for two-photon polymerisation is normally in the range of 50 mW to 75 mW. The sample is later soaked in isopropanol for 3 min to remove any unpolymerised resist. A curing structure made by PEGDA two-photon polymerisation is shown in Figure 3-8. The originally designed structure is a flat sheet. The surface tension induced by isopropanol evaporation leads to the two corners rolling up and touching each other.

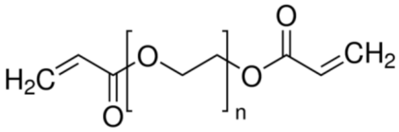

Figure 3-7: The chemical structure of PEGDA.

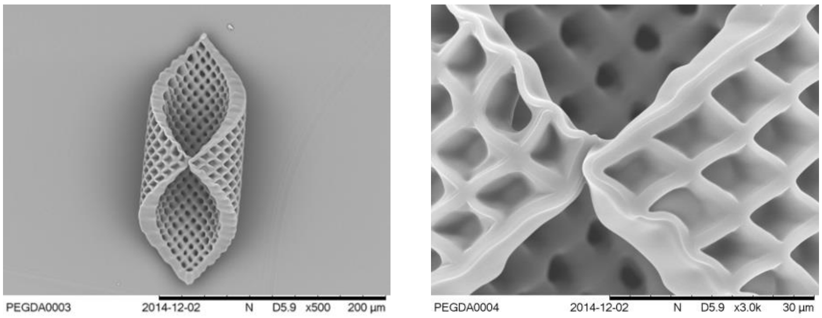

Figure 3-8: SEM images of a curing structure made by PEGDA.

3.6. Fabricate on flexible substrate

All the preliminary work was carried out on glass substrates. In recent years the need for flexible and wearable devices has grown tremendously and tests were performed to ascertain feasibility of fabrication on a flexible substrate. Polyester film is a common substrate used in industry owing to its balanced properties compared to other thermoplastic polymers. As shown in Figure 3-9, OrmoComp micro/nano patterns have been successfully fabricated on polyester films by two-photon polymerisation. A laser power of 23 mW was used and the scanning speed varied from 20 µm/s to 100 µm/s.

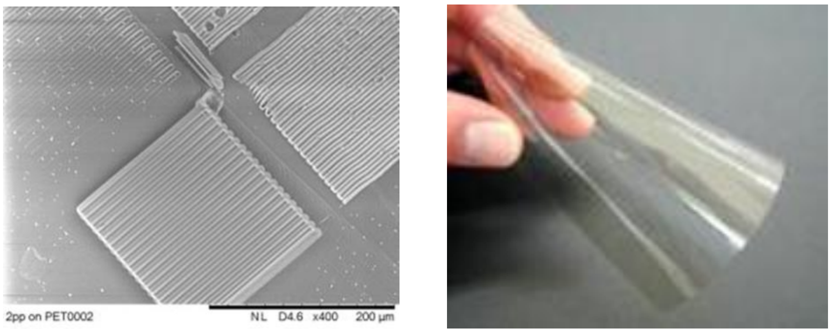

(a) (b)

Figure 3-9: (a) SEM image showing OrmoComp patterns fabricated by two-photon polymerisation on polyester film; (b) Picture showing polyester film with OrmoComp patterns.

4. Two-photon reduction

Both gold and silver micro/nano structures can be fabricated by two-photon induced chemical reduction. As gold is more stable than silver in antioxidation and corrosion as well as its wide application for surface plasmon resonance, gold is preferred in the current study. Gold(III) Chloride Hydrate, $HAuCl_4 \cdot H_2O$, (Sigma-Aldrich) at 0.25 M aqueous solution was used. Au nanoparticles form on the glass substrate after laser scanning, as shown in Figure 4.1. The used laser power ranges between 15 mW to 25 mW. The size of nanoparticles ranges from 40 nm up to 160 nm. For a metal particle to grow, it needs both sufficient photon energy and a sufficient number of metal ions at the laser beam spot. High-intensity laser irradiation expends the ions quickly in the vicinity of laser beam spot, and the resulting lack of metal ions stops further growth of the metal particles. The limited mobility of the ions restricts the supply of the ions diffusing in from the surrounding region, thus determining the size of metal particles. After repeated laser scanning, nanoparticles agglomerate into big clusters. As illustrated in Figure 4-1(a) and 4-2, clusters up to 10 µm are visible. Chemical composition of the big clusters is analysed by Energy-dispersive X-ray spectroscopy (EDX). Both spot analysis and area mapping results are shown in Figure 4-2(b) and (c), confirming the big clusters are composed of Au.

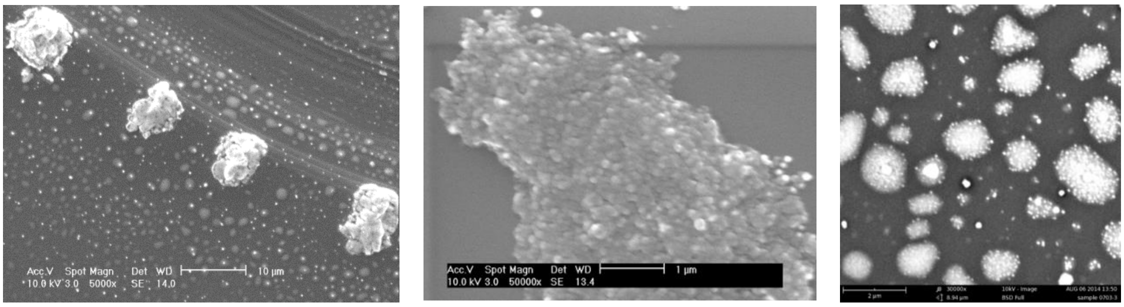

(a) (b) (c)

Figure 4-1: SEM images showing Au nanoparticles and clusters prepared by two-photon induced metal salt reduction

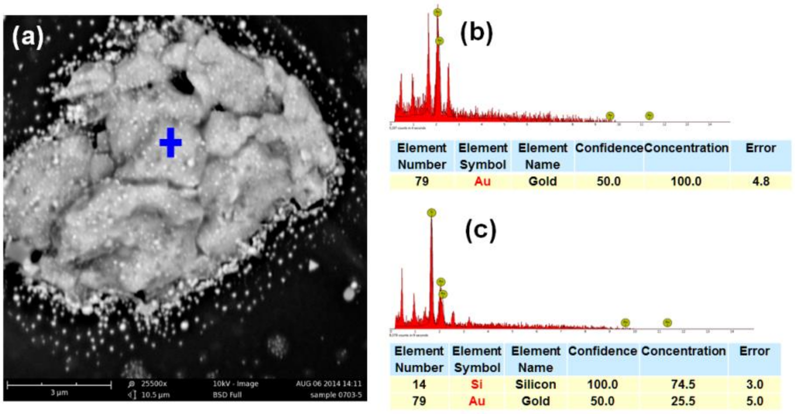

Element Number	Element Symbol	Element Name	Confidence	Concentration	Error
79	Au	Gold	50.0	100.0	4.8

Element Number	Element Symbol	Element Name	Confidence	Concentration	Error
14	Si	Silicon	100.0	74.5	3.0
79	Au	Gold	50.0	25.5	5.0

Figure 4-2: (a) SEM image of an Au cluster; (b) EDX spot analysis at the position marked by a cross in blue in (a); (b) EDX area mapping the big cluster.

5. Combining two-photon polymerisation and photoreduction in a single step

In Work Package 3, it is proposed to process both polymeric and metallic materials simultaneously. This has the objective of demonstrating that the combination of materials is possible whilst also showing the potential for application for metamaterials, where complex material structures that interact with electromagnetic radiation are requird. As a consequence a number of polymer resin and Au salt combinations have been tested for nano-composite fabrication to understand the underlying processes and empirically determine suitable for mixtures. Each combination will be presented and the observations reported in the following sections.

5.1. Commercial polymer resins + Au salt

Possible commercial polymer resins were OrmoComp, SU8 and IPL. However, as Gold(III) chloride hydrate ($HAuCl4·H2O$) is in insoluble OrmoComp, no investigation was undertaken with this combination.

5.1.1. SU8 + Au salt

SU8+Au composites were fabricated by exposing the mixture of SU8 and Au salt to the laser at an energy of 30 mW. A hybrid pattern is shown in Figure 5-1. The grey lines were made of SU8, and the white dots were Au nanoparticle aggregations, with the sizes ranging from dozens of nanometers up to 1 μm. The aggregation of Au nanoparticle in SU8 matrix is more predominant compared to that in IPL matrix (Section 5.1.2. Ionic-based polymerisation (for the case of SU8) tends to generate more heat than radical-based polymerisation (for the case of IPL). The local heat can accelerate the surface diffusion of Au nanoparticles, thus promote aggregation. Therefore for high resolution nano-composite fabrication, radical-based polymerisation is preferred.

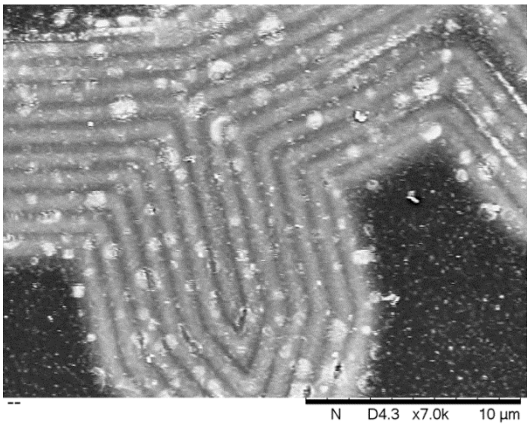

Figure 5-1: SEM image of SU8-Au nano-composite. The grey lines were SU8, and the white dots were Au nanoparticle aggregations.

5.1.2. IPL + Au salt

5.1.2.1. IPL + Au salt

Despite commercial IPL being designed for two-photon processing, no polymerisation was observed for the sample with Au based salt added. As shown in Figure 5-2, only Au nanoparticle aggregation is observed. It is supposed that this was because two-photon induced metal ion reduction consumes free radicals generated by the photoinitiators, which are also required for the polymerisation. This lack of free radicals suppresses the polymerisation and prevents cross-linking. To overcome this, extra photoinitiator was added to the material to promote the formation of polymer alongside the gold nanoparticles.

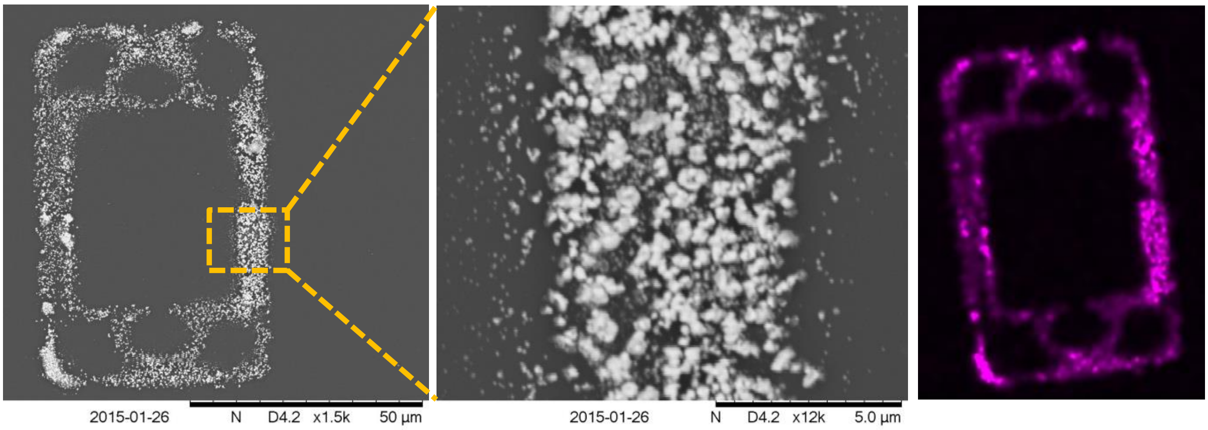

(a) (b) (c)

Figure 5-2: (a) SEM image showing the pattern fabricated by using the mixture of IPL with gold chloride without extra initiators; (b) Magnified SEM image showing the section marked in figure (a); (c) EDX mapping analysis showing the Au element distribution of the pattern shown in figure (a).

5.1.2.2. IPL + Au salt + extra initiator

Extra photoinitiators were added to the mixture of IPL and gold chloride, to provide extra free radicals and promote the two reactions – polymerisation and reduction – to happen at the same time. Rhodamine B and a new photoinititiator, developed in house (known as T3), were tested. The chemical structure of Rhodamine B is given in Figure 5-3.

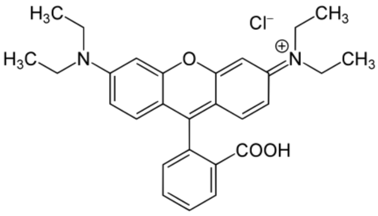

Figure 5-3: Chemical structures of Rhodamine B (CAS: 81-88-9, Sigma-Aldrich 83689).

Rhodamine B was chosen due to its high two-photon absorption (TPA) cross-section at the wavelength of 780 nm - the wavelength of the laser used in this study (Makarov, Drobizhev et al. 2008). Figure 5-4(a) shows a 10-µm-high micro structure formed by adding a small amount of rhodamine B to the mixture of IPL and gold chloride. Its surface morphology looks similar to the structure formed by using pure IPL. However, EDX analysis shows that Au nanoparticles are embedded in the IPL matrix. As shown in Figure 5-4(b), the distribution of Au element corresponds well with the 3D micro structure. However, the distribution of Cl is almost uniform throughout the whole substrate (see Figure 5-4(c)) suggesting that Au has been localised within the polymer matrix.

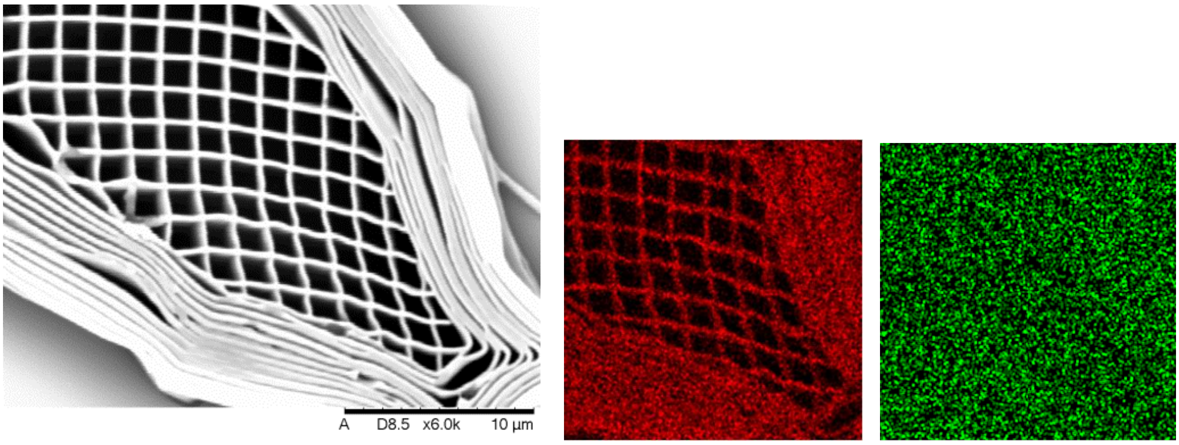

(a) (b) (c)

Figure 5-4: (a) SEM image of IPL-Au nano-composite fabricated using rhodamine B as extra photoinitator. The pattern is about 10 µm high; EDX mapping analysis showing (b) Au distribution and (c) Cl distribution at the right bottom area of the pattern shown in (a).

Two-photon initiators were not commercially available until recently. Interest in this area, however, has led to a series of benzylidene ketone based two-photon initiators becoming available. These low-cost initiators showed good TPA cross sections and hence have great potential for commercialization (Li, Pucher et al. 2013). It was also reported that a cooperative enhancement effect of TPA was observed in dyes with 2 or more branches, resulting in large TPA cross section and high sensitizing efficiency (Wu, Zhao et al. 2006). A modification of this photoinitiator was developed, creating a new 3-branched two-photon initiator T3. Figure 5-5 shows grid patterns fabricated using T3 as extra initiator. Similar to the case with rhodamine B, the generated Au nanoparticles were embedded within the IPL matrix, and no aggregation can be observed by SEM analysis. The combined IPL cross-linking and gold reduction is hypothesized to occur by the mechanism illustrated in Scheme 1.

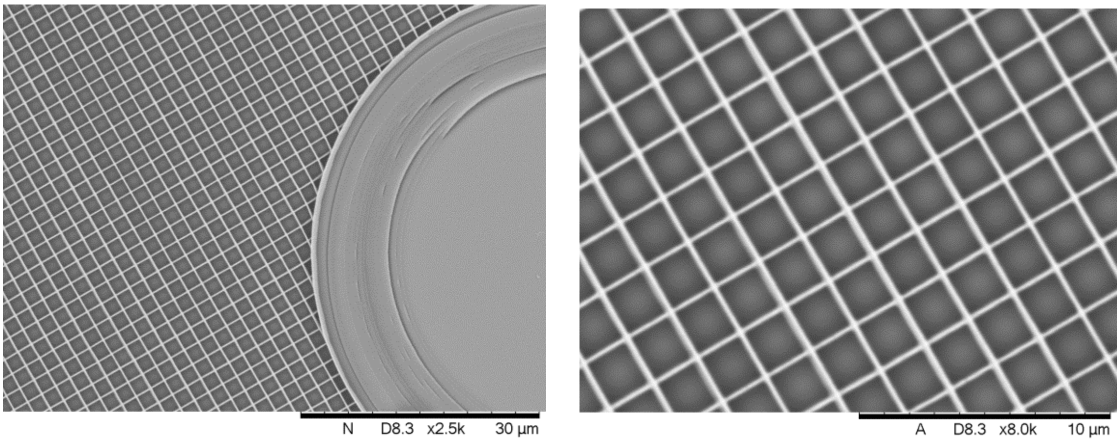

(a) (b)

Figure 5-5: SEM images of IPL and Au nano-composite fabricated using T3 as extra initiator.

Free radicals elimination from two-photon excitation (chain initiation):

$$I \xrightarrow{h\nu} 2R\cdot \qquad (1)$$

Free radical polymerisation (Chain propagation):

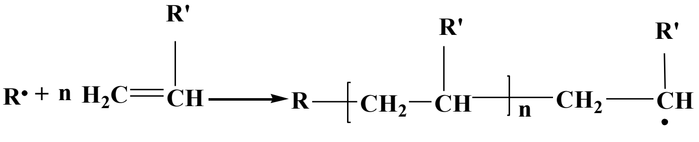

$$R\cdot + n\, H_2C{=}\overset{R'}{\overset{|}{CH}} \longrightarrow R{-}\left[CH_2{-}\overset{R'}{\overset{|}{CH}}\right]_n{-}CH_2{-}\underset{\bullet}{\overset{R'}{\overset{|}{CH}}} \qquad (2)$$

Chain termination:

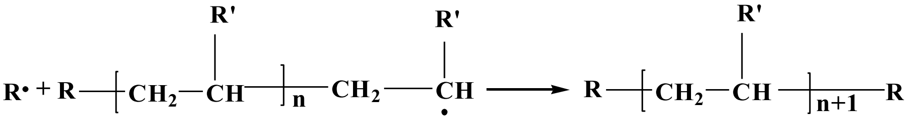

$$R\cdot + R{-}\left[CH_2{-}\overset{R'}{\overset{|}{CH}}\right]_n{-}CH_2{-}\underset{\bullet}{\overset{R'}{\overset{|}{CH}}} \longrightarrow R{-}\left[CH_2{-}\overset{R'}{\overset{|}{CH}}\right]_{n+1}{-}R \qquad (3)$$

Gold reduction from Au^{3+} to Au^{2+}:

$$R\cdot + AuCl_4^- \longrightarrow R^+ + AuCl_3^- + Cl^- \qquad (4)$$

Au^{2+} disproportionation:

$$2AuCl_3^- \longrightarrow AuCl_2^- + AuCl_4^- \qquad (5)$$

Au^{2+} and Au^+ disproportion:

$$AuCl_2^- + AuCl_3^- \longrightarrow AuCl_4^- + Au^0 + Cl^- \qquad (6)$$

Gold nanoparticles aggregation:

$$n\,Au^0 \longrightarrow Au_0$$

(7)

Scheme 1: Proposed mechanism of simultaneous photopolymerisation and photoreduction.

The photoinitiator T3 has a large TPA cross section and high sensitizing efficiency, but its solubility in ethanol is limited, which constrains the amount that can be added to the mixture of monomer and Au salt. The nanocomposite shown in Figure 5-5 was fabricated using 98.7 wt% IPL, 1.2 wt% Au salt and 0.1 wt% T3. When the Au salt concentration is raised, polymerisation is not triggered. One example is shown in Figure 5-6, which was fabricated using 96 wt% IPL, 3 wt% Au salt and 0.1 wt% T3. When the amount of Au salt was increased to 5 wt%, no polymerisation was observed. This could be associated with two reasons: a) There is insufficient initiator to promote both polymerisation and photoreduction to happen at the same time; b) Components within the commercially hidden formulation may conflict with the extra initiator T3. For this reason, further work in this section focused on non-commercial blends.

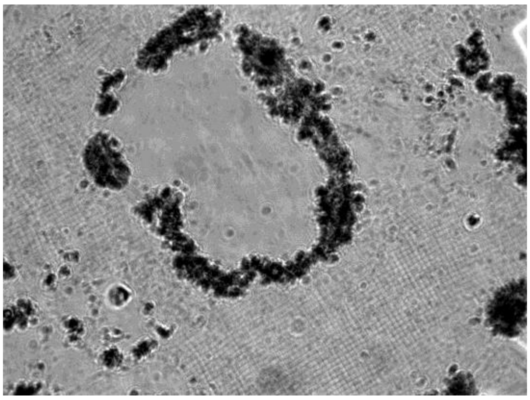

Figure 5-6: Optical microscope image showing partial polymerisation and Au salt reduction by using the mixture of 96 wt% IPL, 3 wt% Au salt and 0.1 wt% T3. The black area is accumulation of Au particles.

5.2. In-house formulated mixtures

Using commercial polymer resins has the advantage of convenience. However, as suppliers are normally unwilling to release the complete chemical formulas to customers, it is difficult to adjust them for other applications. Here we demonstrate another route for fabricating composites using pure monomer and known initiators.

5.2.1. TMPTA + Au salt

Trimethylolpropane triacrylate (TMPTA) (CAS: 15625-89-5, Sigma-Aldrich) is chosen as the monomer. It is the main monomer used in OrmoComp, as illustrated in Figure 5-7(a). Photoinitiator 2-Benzyl-2-(dimethylamino)-4’-morpholinobutyrophenone (DBMP) (CAS: 119313-12-1, Sigma-Aldrich) and photocatalyst Ruthenium-tris(2,2’-bipyridyl) dichloride (Ru(II)) (CAS: 50525-7-4, Sigma-Aldrich) were tested. Their chemical structures are shown in Figure 5-7(b) and (c).

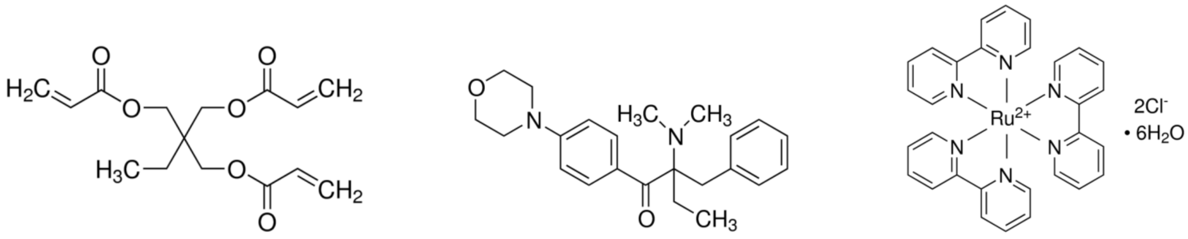

(a) (b) (c)

Figure 5-7: Chemical structures of tested (a) monomer TMPTA, (b) photoinitiator DBMP and (c) photocatalyst Ru(II).

As mentioned previously, polymer cross-linking and metal ion reduction are two competing processes as free radicals are needed in both reactions. The lacking of sufficient free radicals can cause one of these processes to be suppressed. Increasing the ratio of gold chloride in the mixture often leads to no polymerisation. In the current study, to keep both polymerisation and reduction processing at the same time, the amount of Au salt was kept to less than 5 wt%. Photoinitiators can promote the generation of free radicals, and thus can help to adjust the competition between processes. The quality of produced composite also depends on the ratio of each component in the mixture. Figure 5-8 shows two TMPTA-Au composite samples generated under different chemical ratios: (a) with 3 wt% Au salt and 3 wt% DBMP; (b) with 5 wt% Au salt and 5 wt% DBMP.

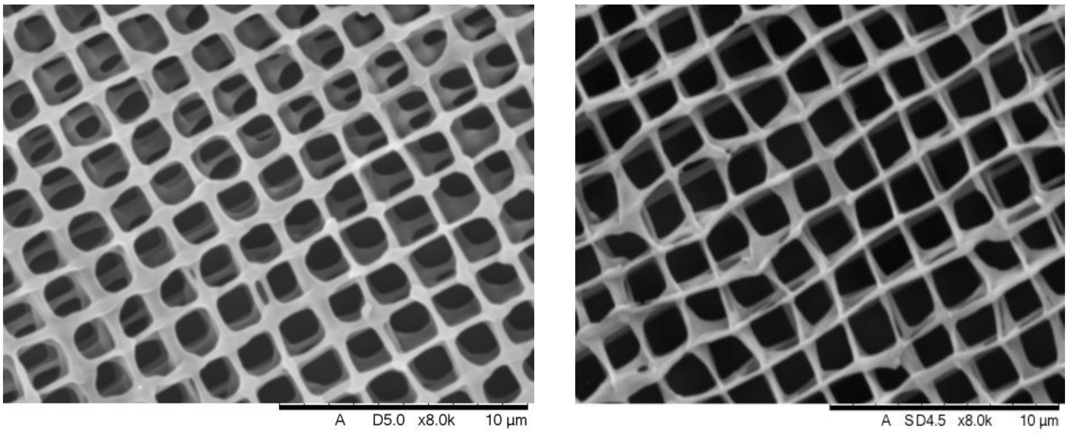

(a) (b)

Figure 5-8: SEM images of TMPTA and Au nano-composite fabricated using DBMP as initiator: (a) The mixture has 3 wt% Au salt and 3 wt% DBMP; (b) The mixture has 5 wt% Au salt and 5 wt% DBMP.

The quality of the TMPTA-Au nano-composite can be improved by adding 0.1 wt% of Ru(II) in the formulation. One example is shown in Figure 5-9, which was fabricated using the mixture of 93.9 wt% TMPTA, 3 wt% Au salt, 3 wt% DBMP and 0.1 wt% Ru(II). Ru(II) complex as a photoncatalyst has been studied recently (Sauvage, Collin et al. 1994; Vurth, Baldeck et al. 2008). The transition metal complexes of Ru(I) and Ru(II) have played a key role in photophysics and photochemistry. The strong light absorption of $Ru(bpy)_3^{2+}$ makes a lowest excited state based on a dπ(Ru)→ π *$(bpy)_3^{2+}$ singlet metal-to-ligand charge transfer (MLCT) state which has long lifetime. The MLCT state is generally inert to photosubstitution so it can withstand long-term photolysis and undergo facile electron and energy transfer. The yields $[Ru^{III}(bpy)_3]^{3+}$ are formed after two photons are absorbed simultaneously resulting in the photoejection of an electron, as illustrated in Scheme 2.

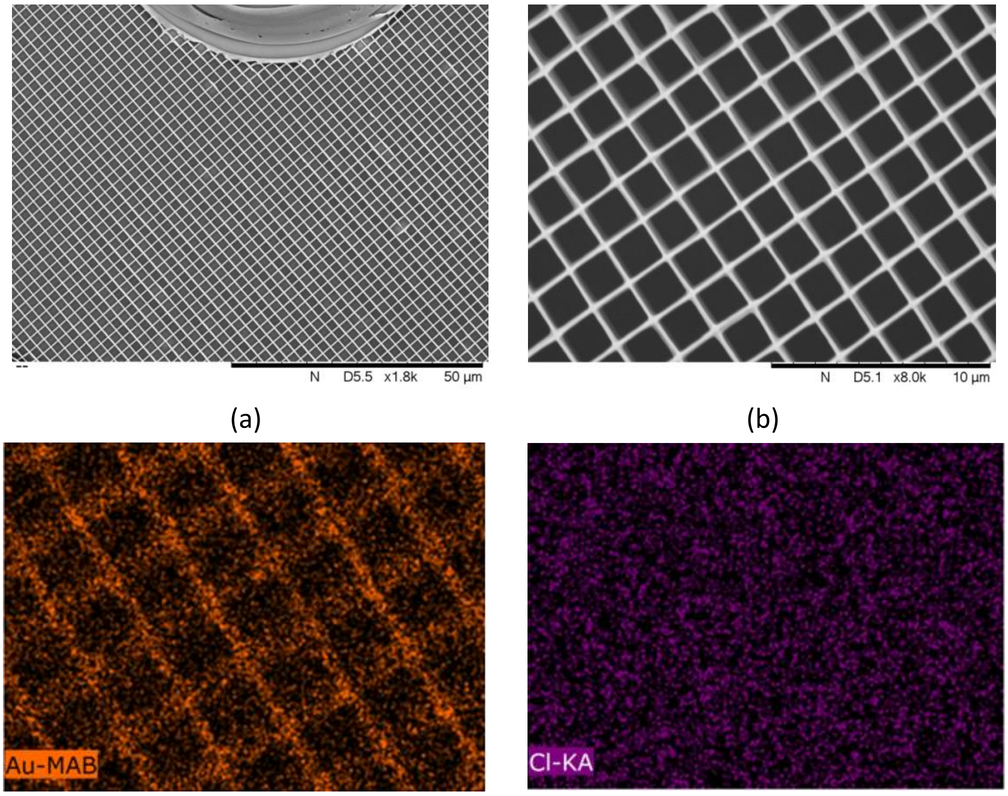

(a) (b)

(c) (d)

Figure 5-9: (a)-(b): SEM images of TMPTA and Au nano-composite fabricated using DBMP as initiator and Ru(II) as catalyst. EDX mapping analysis showing (c) Au distribution and (d) Cl distribution for the pattern shown in (b).

$$[Ru^{II}(bpy)_3]^{2+} \overset{h\nu}{\rightarrow} [Ru^{III}(bpy^{\cdot-})(bpy)_2]^{2+} \overset{h\nu}{\rightarrow} [Ru^{III}(bpy)_3]^{3+} + e_{aq}^{-} \qquad (8)$$

$$[Ru^{II}(bpy)_3]^{2+} + e_{aq}^{-} \rightarrow [Ru^{II}(bpy^{\cdot-})(bpy)_2]^{+} \qquad (9)$$

$$2\,[Ru^{III}(bpy^{\cdot-})(bpy)_2]^{2+} \rightarrow [Ru^{II}(bpy^{\cdot-})(bpy)_2]^{+} + [Ru^{III}(bpy)_3]^{3+} \qquad (10)$$

Scheme 2: Proposed transaction after two-photon absorption.

5.2.2. PETA + Au salt

Pentaerythritol triacrylate (PETA) (CAS: 3524-68-3, Sigma-Aldrich) is the monomer used in IPL, with its chemical structure shown in Figure 5-10. Here we mixed PETA with Au salt and initiator DBMP. Nano-composite structures fabricated with and without Ru(II) are compared in Figure 5-11. Both samples contain 3 wt% Au salt and 3 wt% DBMP. Structures shown in Figure 5-11 (c) and (d) also contain 0.1 wt% Ru(II). The mechanism of Ru(II) in maintaining the shape of the structures is not clear and needs further investigation.

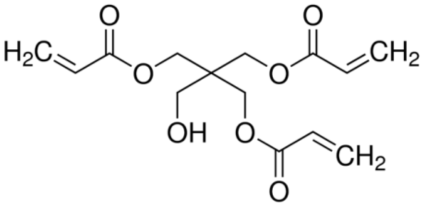

Figure 5-10: Chemical structure of PETA.

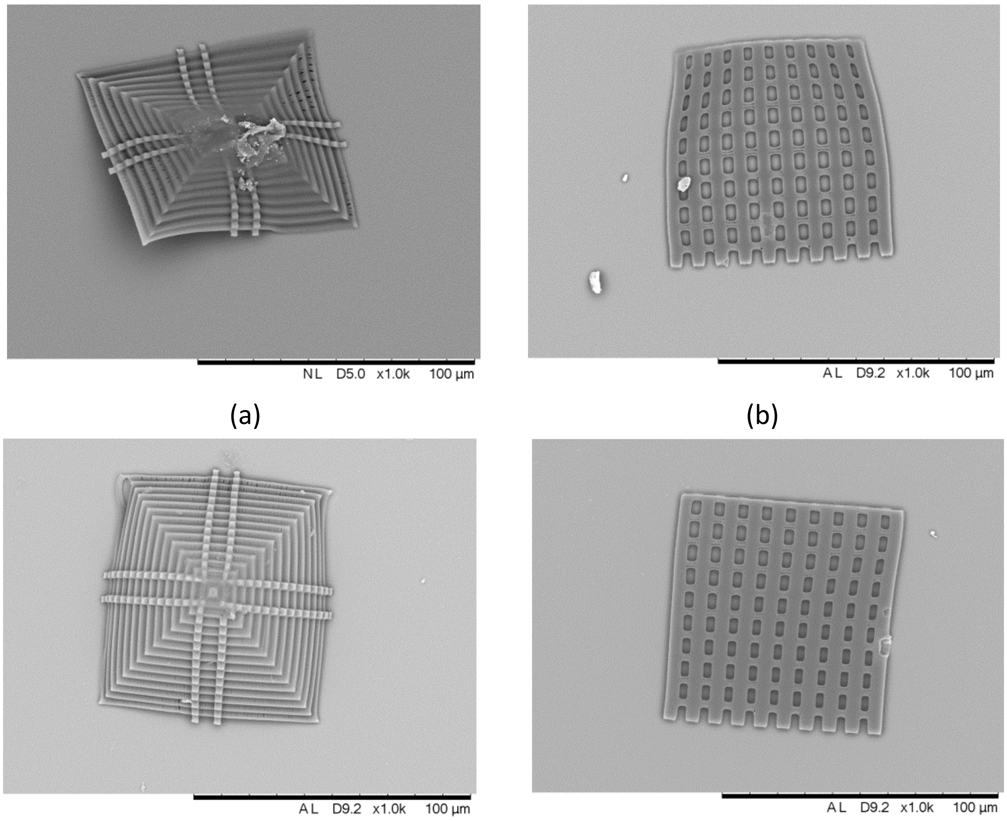

(a) (b)

(c) (d)

Figure 5-11: SEM images showing PETA-Au nano-composites fabricated using (a)-(b) 94 wt% PETA, 3 wt% Au salt and 3 wt% DBMP, (c)-(d) 93.5 wt% PETA, 3 wt% Au salt, 3 wt% DBMP and 0.1 wt% Ru(II).

6. Controlling two-photon polymerisation and photoreduction in a single step

It is proposed that the addition of another laser source with the potential to suppress polymerisation or reduction will enable independent control of both of these processes. Two sources were used - a 780 nm fs laser and a 532 nm CW laser. The setup is illustrated in Figure 6-1. Two of the mixtures formula developed in Section 5 were tested – the commercial IPL with Au salt and in-house formulated PETA with Au salt.

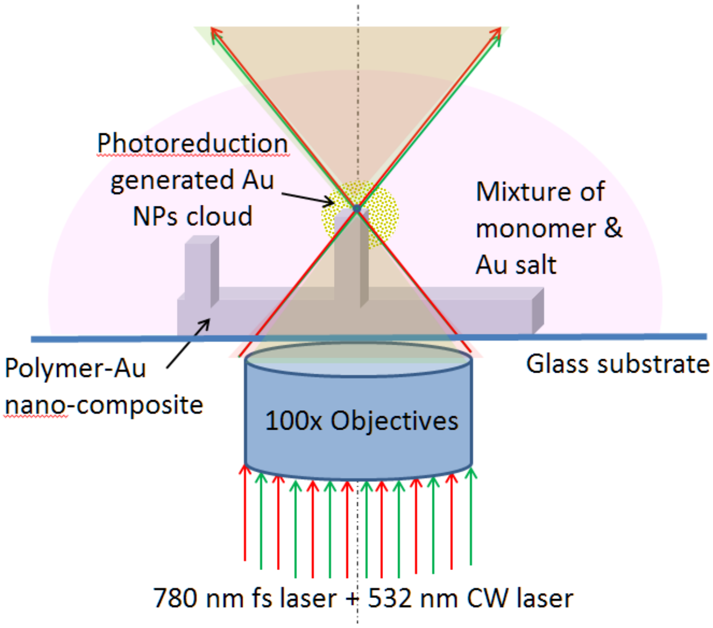

Figure 6-1: Illustration showing the setup for the two-laser system.

6.1. Polymerisation enhancement

When the supplementary 532 nm laser was added to the system, polymerisation enhancement was observed for the fabrication of IPL-Au nano-composites and PETA-Au nano-composites. Figure 6-2 shows some examples. For the purpose of comparison, area A in Figure 6-2(c) and areas C & E in Figure 6-2(e) were fabricated using the near-IR fs laser alone, while the rest of the areas were fabricated using both the near-IR fs laser and the green (532 nm) CW laser simultaneously. The laser power and scanning speed were kept the same within a single pattern. Area F in Figure 6-2(e) has an additional layer (repeated scanning at elevated height) compared to the number of layers for area D. The change of surface morphology between area A and B is clear – the green laser leads to enhanced polymerisation. This phenomenon can also be observed in Figure 6-2(e) when comparing area C/E with area D/F.

The formed patterns by the two-laser system are composites. Similar to the case of fabricating with near-IR fs laser alone (see Section 5), locally generated Au nanoparticles are embedded in polymeric patterns. The successful Au salt reduction is demonstrated by the uniform distribution of Cl elements and non-uniform distribution of Au elements, as shown in Figures 6-2(f) and (g) through EDX mapping analysis. The concentration of Au nanoparticles in polymeric patterns fabricated by the two lasers is higher than that of one laser, as demonstrated in Figure 6-2(d) and (f). This difference demonstrates that the two-laser system can be used to control Au concentration in nano-composites.

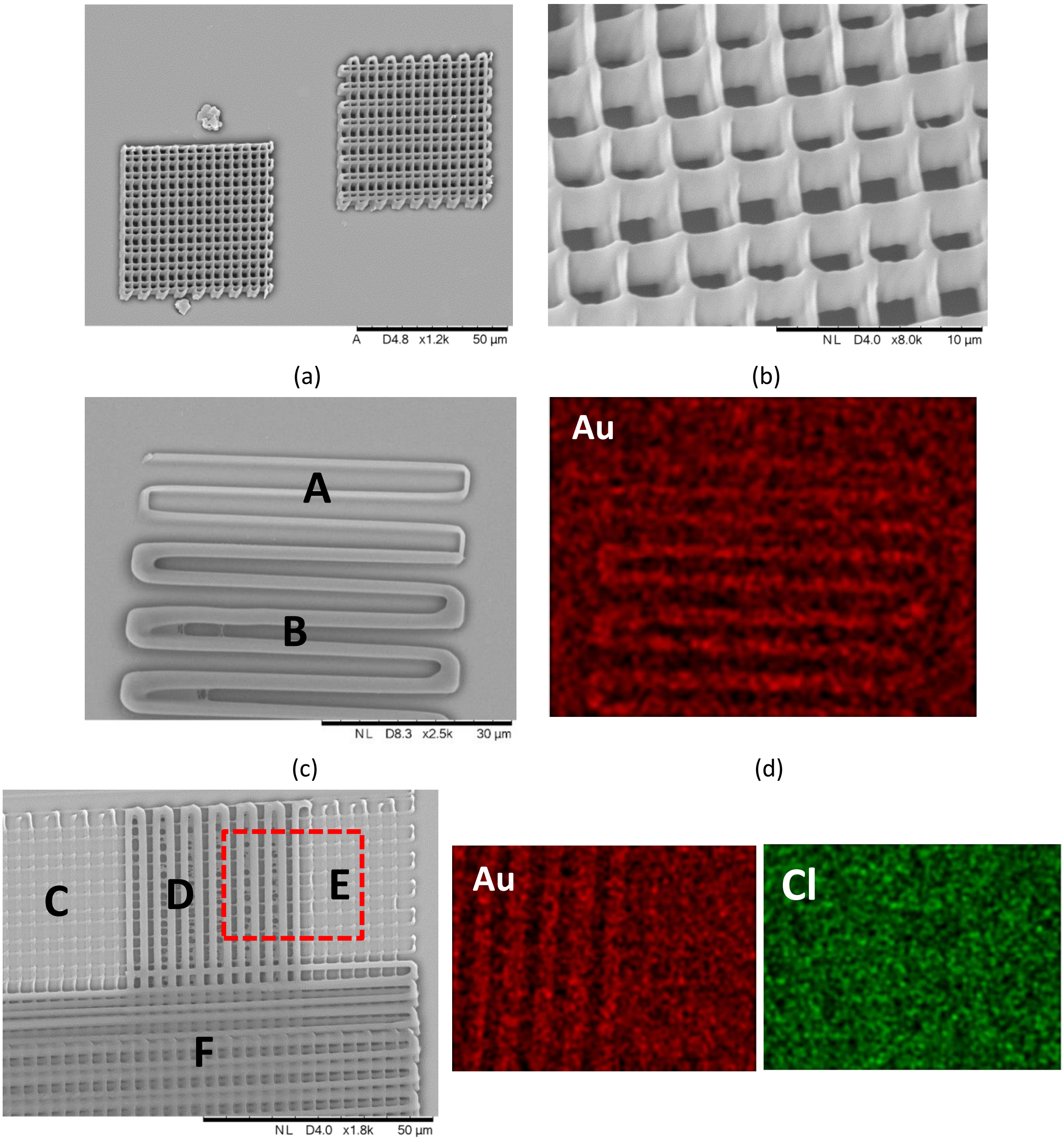

(a) (b)

(c) (d)

(e) (f) (g)

Figure 6-2: SEM images showing (a) IPL-Au nano-composite fabricated using 99.1 wt% IPL, 0.8 wt% Au salt and 0.1 wt% T3; (b), (c) &(e) PETA-Au nano-composite fabricated using 94 wt% PETA, 3 wt% Au salt and 3 wt% DBMP. Area A, C and E were fabricated using the near-IR fs laser alone, and the rest areas were fabricated by firing both the near-IR laser and the green laser at the same time; (d)

EDX mapping analysis showing the distribution of Au in the area shown in figure (c); (f) EDX mapping analysis showing the distribution of (f) Au and (g) Cl in the area marked by dash lines in figure (e).

To identify the role of the green laser in nano-composite fabrication, comparison tests were carried out using the green laser alone on pure polymer sample and polymer-Au mixed sample. Figure 6-3(a) show an optical microscope image taken directly after the green laser scanning on pure polymer sample (with 97 wt% monomer PETA and 3 wt% initiator DBMP) at an energy of 30 mW. No change of surface morphology was observed. Although it is possible for pure monomer polymerisation by green laser alone (Thiel, Fischer et al. 2010), the laser power used in current study is lower than the threshold for polymerisation. However, scanning the green laser at the same energy and the same scanning speed can lead to polymerisation on PETA-Au sample (with 97 wt% PETA, 3 wt% Au chloride hydrate and 3 wt% DBMP). This phenomenon implies that the presence of Au salt, or perhaps the generation of Au nanoparticles, can lower the threshold for monomer polymerisation. The mechanism is not clear and needs further investigation.

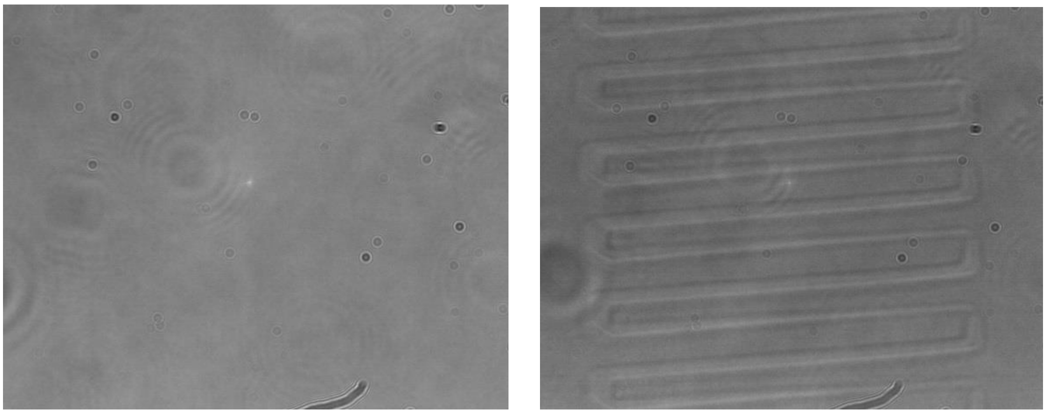
(a) (b)

Figure 6-3: (a) Optical microscope image of the PETA sample (with 97 wt% monomer PETA and 3 wt% initiator DBMP) after exposure to the 532 nm CW laser at energy of 30 mW and scanning speed of 20 μm/s; (b) Optical microscope image of the PETA-Au sample (with 97 wt% PETA, 3 wt% Au chloride hydrate and 3 wt% DBMP) after exposure to the same laser at the same energy and the same scanning speed.

6.2. Polymerisation inhibition

Polymerisation inhibition based on stimulated emission depletion on pure polymer sample has been reported before (Fischer and Wegener 2012). In current study, so far we have not observed the inhibition on composite sample. The inhibition is dependent on the precise details of the electron energy levels within the photoinitiator and the tendency for the elevated energy state to transition through intersystem crossing and subsequent chemical changes and that in our case, the interaction between the green laser and the photoinitiator is not sufficiently well tuned to be able to suppress polymerisation. Further work to understand this process is required.

6.3. Photoreduction enhancement

A form of enhanced photoreduction has been observed on composite samples by using the green CW laser alone. Figure 6-4 shows optical microscope images taken directly after laser exposure. In each image, the upper part of the area was scanned by the near-IR laser alone, and the lower part of the area was scanned by the green laser alone. The energy of the near-IR laser was kept at 50 mW, and the energy of the green laser was (a) 16 mW, (b) 12.5 mW, (c) 8 mW and (d) 4 mW, respectively. In the lower part of each image, photoreduction generated a cloud of Au nanoparticles that are distinct from the polymerised material. This phenomenon can be enhanced by the increase of the green laser energy. In comparison to the photoreduction generated by the near-IR laser, the threshold for photoreduction by the green laser is much lower, around 5 mW compared to 15 mW. No cloud phenomenon is observed when the near-IR fs laser is used. It is supposed that this is a result of the non-linearity in the multiphoton absorption. Variations in the shape of the cloud are likely due to agitation during movement of the sample whilst fabricating.

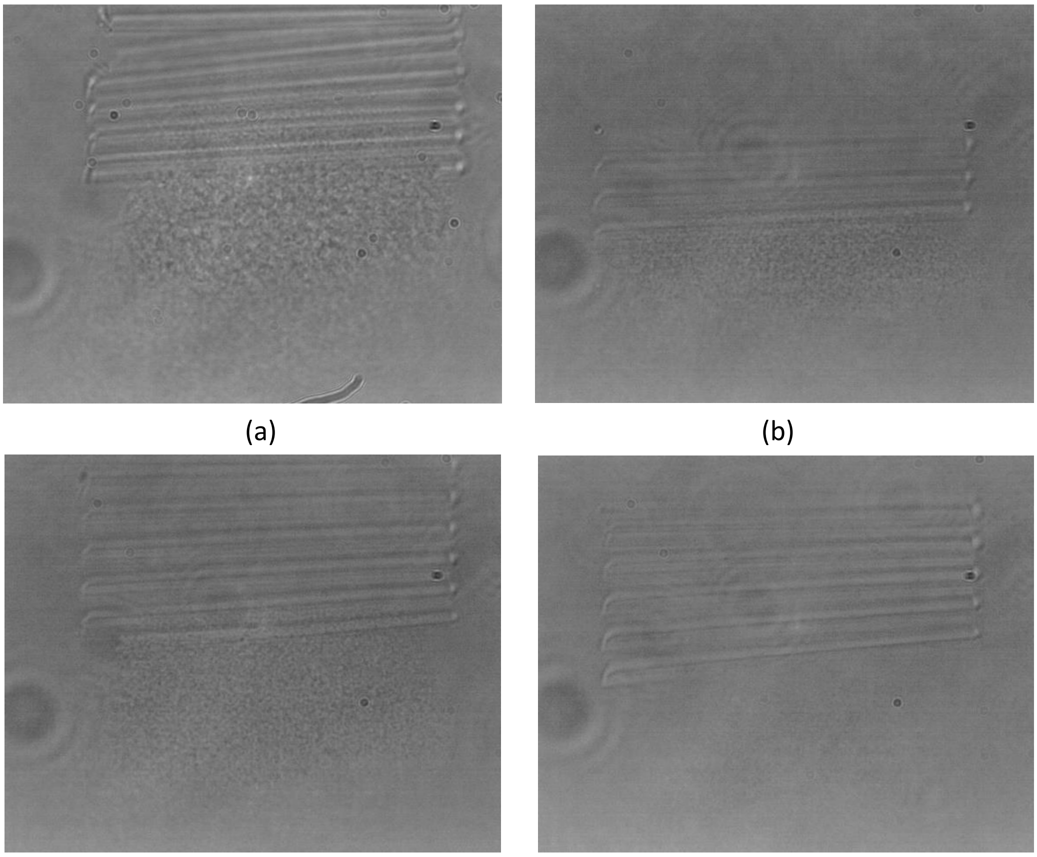

(a) (b)

(c) (d)

Figure 6-4: Optical microscope images taken after laser exposure. In each image, the upper part of the area was scanned by near-IR laser alone at 50 mW, and the lower part of the area was scanned by green laser alone at various energies: (a) 16 mW, (b) 12.5 mW, (c) 8 mW and (d) 4 mW.

The enhanced photoreduction can also be observed when both lasers were fired at the same time. Figure 6-5 shows an optical microscope image taken on a PETA-Au sample after exposure to the near-IR laser at 53 mW and the green laser at 11 mW at the same time. Besides forming PETA polymer matrix blended with freshly generated Au nanoparticles, excess Au nanoparticles floated like a cloud on top of the nano-composite pattern. Most of the suspended Au nanoparticles can be removed later in the sample development procedure, whilst some precipitate in the surrounding area. This could affect the Au distribution examined by EDX, leading to strong background signals of Au, as shown in Figures 6-2(d) and (f).

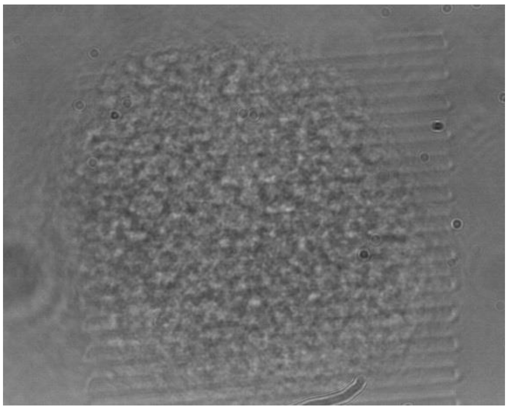

Figure 6-5: Optical microscope image showing the PETA-Au sample after exposure to both the near-IR laser at 53 mW and the green laser at 11 mW at the same time.

The presence of the Au nanoparticle cloud induced by the green CW laser opens a route for tuning the Au concentration in composites. After the formation of the nanoparticle cloud, if the near-IR fs laser is used to scan at the cloudy area, it is possible to blend the Au nanoparticles in the formed structure. One example is shown in Figure 6-6. The first layer was fabricated by scanning both lasers at the same time, as shown in Figure 6-6(a). The second, third and fourth layer were fabricated by scanning the near-IR fs laser alone at the cloudy area, as shown in Figures 6-6(b)-(d). As Au can absorb laser energy, overheating induced burning can often be observed when multi-layer structure is fabricated, leading to the black area shown in Figures 6-6(c) and (d). The burning actually implies the possible high concentration of Au. The white dots shown in Figure 6-6(c) are probably formed from Au nanoparticles in the cloud. Further investigation is needed to find the optimized laser energy and scanning speed to avoid the local burning.

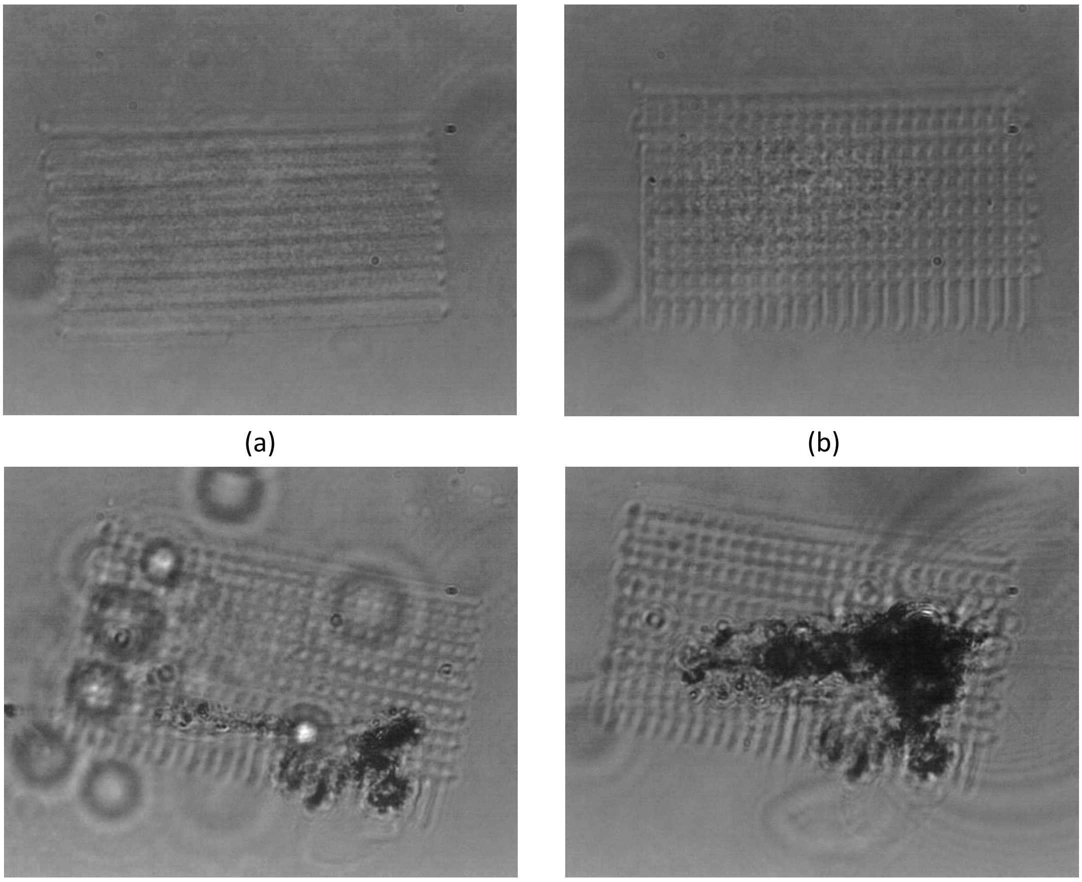
(a) (b)

(c) (d)

Figure 6-6: Optical microscope images showing (a) the first layer, (b) the second layer, (c) the third layer and (d) the fourth layer in nano-composite fabrication.

In summary, using the mixture formula discussed in Section 5, the functions of the near-IR fs laser and the green CW laser in polymer fabrication and polymer-Au nano-composites fabrication are summarized in Table 6-1. Compared to using the near-IR fs laser alone (see Section 5 for detail), the addition of the green CW laser can lead to enhanced polymerisation and enhanced photoreduction. The photoreduction enhancement can be used to tune the Au concentration in the fabricated polymer-Au nano-composites.

Table 6-1: Summary of the functions of 780 nm fs laser and 532 nm CW laser

Sample **Power source**	**Polymer resin**	**Mixture of polymer resin & Au salt**
780 nm fs laser	Polymerisation	Polymerisation + photoreduction
532 nm CW laser	N/A	Photoreduction Polymerisation (at sufficient high energy)
780 nm fs laser + 532 nm CW laser	Enhanced polymerisation	Enhanced polymerisation + enhanced photoreduction

7. Future applications and future work

The technology developed in current study has great potential in various applications, such as metamaterials, plasmonics, and nanophotonics. Some potential some metamaterial-based periodic structures are shown in Figure 7-1. Our next step is to characterize their optical and electromagnetic properties.

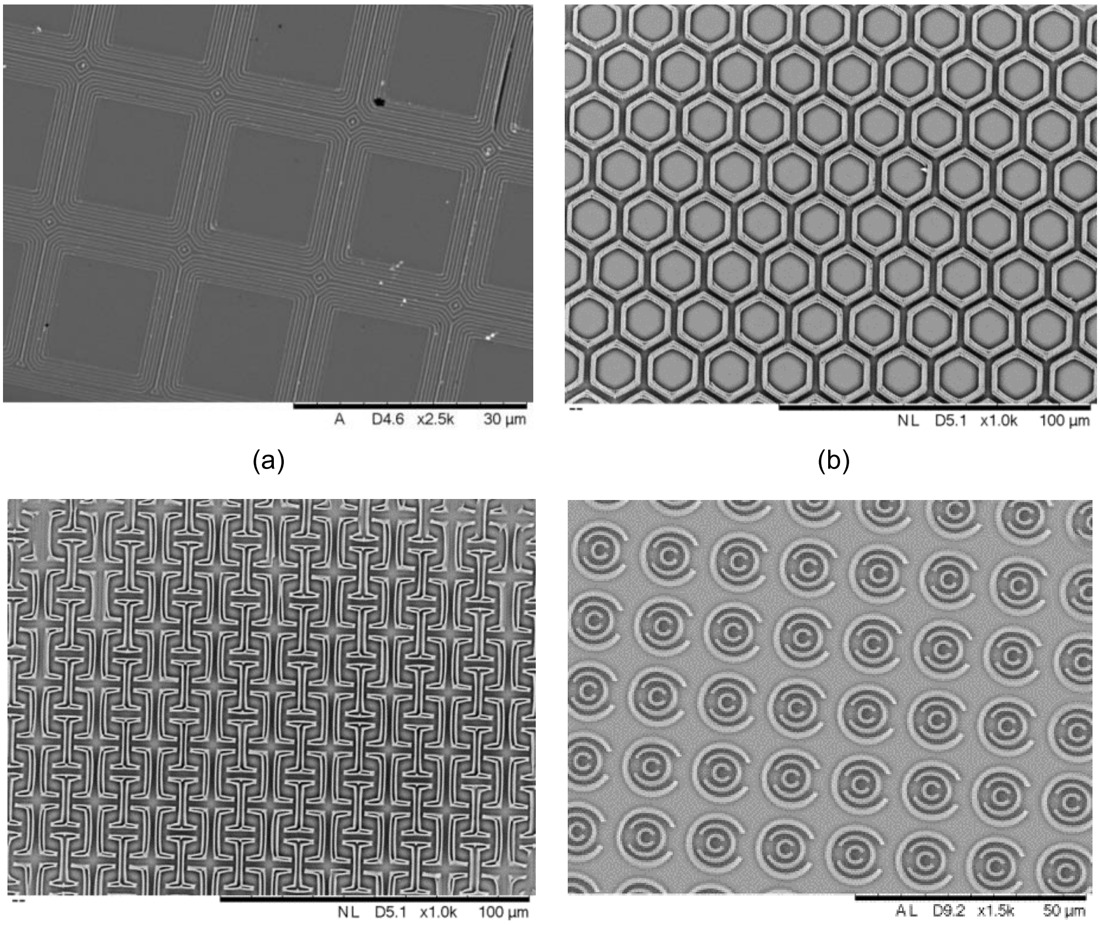

(a) (b)

(c) (d)

Figure 7-1: (a)-(c) SEM images of TMPTA-Au nano-composite periodic structures fabricated using 93.9 wt% TMPTA, 3 wt% gold chloride, 3 wt% DBMP and 0.1 wt% Ru(II); (d) SEM image of PETA-Au nano-composite periodic structures fabricated using 93.9 wt% PETA, 3 wt% gold chloride, 3 wt% DBMP and 0.1 wt% Ru(II).

The proposed future work includes:

- Achieving polymerisation inhibition on a composite sample. One possible route is by using different initiators, such as DETC. Modifying the current two-laser setup is also essential.

- The presence of Au nanoparticle cloud induced by the green CW laser opens a route for tuning the Au concentration in composites. The next step is to develop a strategy to control the concentration and distribution of Au nanoparticles in the process of building additional polymeric layers in close proximity to the Au cloud.

- Increase the amount of Au allowable in nano-composite fabrication. Currently the maximum amount of Au salt in the mixture is 3 wt%. For some applications such as electronics, higher load of Au is needed. One possible route is by adding different or extra initiators in the mixture.

8. Summary of deliverables

This project has made the following deliverables:

D1.1	Determine suitable materials	Complete
D1.2	Construct 2PP system	Complete
D2.1	Demonstration of polymeric structures	Complete
D2.2	Demonstration of metallic structures	Complete
D3.1	Single process multimaterial fabrication	Simultaneous fabrication of polymer and metals – Complete Selective fabrication of polymer and metals – Methods for control established
D3.2	Report	Complete
D3.3	Publications	Three publications under preparation

Major advances resulting from the funding are detailed below:

- A rig for both two-photon polymerisation and photoreduction has been built and tested.
- Two-photon polymerisation using four different resins (OrmoComp, IPL, SU8 and PEGDA), based on different polymerisation mechanisms, have been successfully demonstrated. The tested polymer resin includes both commercial resins and resins developed in our lab Including hard materials and hydrogels.
- Two-photon polymerisation on hard substrates (cover glass) and flexible substrates (polyester film) have both been successfully demonstrated.
- Two-photon induced Au salt reduction has been successfully demonstrated.

- Combining two-photon polymerisation and photoreduction in a single process have been successfully demonstrated.
- Four nano-composites have been successfully fabricated in a single process: SU8-Au, IPL-Au, TMPTA-Au and PETA-Au, using either commercial resin to mix with Au salt (with/without extra initiators), or using in-house formulated mixtures.
- High efficient three-branched photoinitiator T3 has been synthesized and successfully used in nano-composites fabrication.
- Four photoinitiators – Rhodamine B, T3, DBMP and Ru(II) – have been tested and successfully used in nano-composites fabrication.
- Two in-house formulated mixturse – TMPTA + Au salt & PETA + Au salt – have been developed and demonstrated better quality in complex 3D micro structure fabrication than the mixture containing commercial resin and Au salt.
- Early results in controlled and selective two-photon polymerisation and photoreduction in a single process have been demonstrated – the concentration of Au nanoparticles in polymeric patterns can be increased by simultaneous exposure to two laser beams (780 nm fs laser & 532 nm CW laser), compared to that exposure to only one laser beams (780 nm fs laser).
- Polymer-Au periodic micro structures for potential use as metamaterials have been fabricated.
- Future applications and future work have been identified.

The following conference publications have been delivered:

- ‘3D micro/nano fabrication by multiphoton lithography’, poster presentation at the 3rd Annual EPSRC Manufacturing the Future Conference, 23~24 Sept 2014, Glasgow
- ‘Fabrication arbitrary 3D micro/nano structures by multi-photon lithography’, oral presentation at the international conference on small science, 8~11 Dec 2014, Hong Kong (**Invited**)
- ‘Multiphoton lithography based 3D micro/nano printing’, oral presentation at the 2nd Mexican Workshop for Additive Manufacturing, 2~4 June 2014, Queretaro, Mexico (**Invited**)
- ‘Fabrication of 3D polymer-metal nano-composites in a single step by two-photon induced polymerisation and metal salt reduction’, oral presentation at the International Solid Freeform Fabrication Symposium an Additive Manufacturing Conference, 10~12 August 2015, Austin, US
- ‘3D printing polymer-metal nano-composites’, oral presentation at Nanoscribe User Meeting, 6~7 Oct 2015, Eggenstein-Leopoldshafen, Germany

Three journal papers are in drafting stage:

- ‘Direct laser writing of 3D polymer-Au nano-composites’
- ‘Role of 532 nm continuous-wave laser in the process of simultaneous two-photon polymerisation and photoreduction for nano-composite fabrication’

- ‘A comparison of effective initiators for simultaneous two-photon polymerisation and photoreduction during nanocomposite fabrication’

References

Cao, Y. Y., N. Takeyasu, et al. (2009). "3D Metallic Nanostructure Fabrication by Surfactant-Assisted Multiphoton-Induced Reduction." Small **5**(10): 1144-1148.

Cumpston, B. H., S. P. Ananthavel, et al. (1999). "Two-photon polymerization initiators for three-dimensional optical data storage and microfabrication." Nature **398**(6722): 51-54.

Fischer, J. and M. Wegener (2012). "Ultrafast Polymerization Inhibition by Stimulated Emission Depletion for Three-dimensional Nanolithography." Advanced Materials **24**(10): OP65-OP69.

Houbertz, R., S. Steenhusen, et al. (2010). Two-Photon Polymerization of Inorganic-Organic Hybrid Polymers as Scalable Technology Using Ultra-Short Laser Pulses. Coherence and Ultrashort Pulse Laser Emission. F. J. Duarte, InTech**:** 583-608.

Jung, B. J., H. J. Kong, et al. (2011). "Autofocusing method using fluorescence detection for precise two-photon nanofabrication." Optics Express **19**(23): 22659-22668.

Li, Z. Q., N. Pucher, et al. (2013). "A Straightforward Synthesis and Structure-Activity Relationship of Highly Efficient Initiators for Two-Photon Polymerization." Macromolecules **46**(2): 352-361.

Makarov, N. S., M. Drobizhev, et al. (2008). "Two-photon absorption standards in the 550-1600 nm excitation wavelength range." Optics Express **16**(6): 4029-4047.

Manhart, J., K. H. Kunzelmann, et al. (2000). "Mechanical properties of new composite restorative materials." Journal of Biomedical Materials Research **53**(4): 353-361.

Pawlicki, M., H. A. Collins, et al. (2009). "Two-Photon Absorption and the Design of Two-Photon Dyes." Angewandte Chemie-International Edition **48**(18): 3244-3266.

Sauvage, J. P., J. P. Collin, et al. (1994). "Ruthenium(II) and Osmium(II) Bis(terpyridine) Complexes in Covalently-Linked Multicomponent Systems: Synthesis, Electrochemical Behavior, Absorption Spectra, and Photochemical and Photophysical Properties." Chemical Reviews **94**(4): 993-1019.

Thiel, M., J. Fischer, et al. (2010). "Direct laser writing of three-dimensional submicron structures using a continuous-wave laser at 532 nm." Applied Physics Letters **97**(22): 221102.

Vurth, L., P. Baldeck, et al. (2008). "Two-photon induced fabrication of gold microstructures in polystyrene sulfonate thin films using a ruthenium(II) dye as photoinitiator." Applied Physics Letters **92**(17).

Wu, J., Y. X. Zhao, et al. (2006). "Multibranched benzylidene cyclopentanone dyes with large two-photon absorption cross-sections." New Journal of Chemistry **30**(7): 1098-1103.

Wu, S. H., J. Serbin, et al. (2006). "Two-photon polymerisation for three-dimensional micro-fabrication." Journal of Photochemistry and Photobiology a-Chemistry **181**(1): 1-11.

Xu, B. B., H. Xia, et al. (2010). "Flexible Nanowiring of Metal on Nonplanar Substrates by Femtosecond-Laser-Induced Electroless Plating." Small **6**(16): 1762-1766.

Zhou, W. H., S. M. Kuebler, et al. (2002). "An efficient two-photon-generated photoacid applied to positive-tone 3D microfabrication." Science **296**(5570): 1106-1109.

AFOSR Deliverables Submission Survey

Response ID:5656 Data

1.

1. Report Type

Final Report

Primary Contact E-mail
Contact email if there is a problem with the report.

matthew.snyder.2@us.af.mil

Primary Contact Phone Number
Contact phone number if there is a problem with the report

314-235-6420

Organization / Institution name

University of Nottingham

Grant/Contract Title
The full title of the funded effort.

Nanoscale manufacturing by combining two-photon polymerization and photoreduction

Grant/Contract Number
AFOSR assigned control number. It must begin with "FA9550" or "F49620" or "FA2386".

FA9550-14-1-0048

Principal Investigator Name
The full name of the principal investigator on the grant or contract.

Ricky Wildman

Program Manager
The AFOSR Program Manager currently assigned to the award

Matt Snyder

Reporting Period Start Date

1/15/2014

Reporting Period End Date

7/15/2015

Abstract

In this project, we investigated the feasibility of a new method of manufacturing metamaterials by combining two-photon polymerisation (2PP) and photoreduction. A new rig has been built for this purpose. The polymerisation of four materials, OrmoComp, SU8, IPL and PEGDA, based on different polymerisation mechanisms, has each been investigated. Au salt photoreduction has been demonstrated. Polymer-metal hybrid two-photon processing has been tested by mixing each of the four polymers with Au salt. The formulations for simultaneous polymerisation and reduction have been optimised, and methods for controlling each process independently have been explored. The use of a 532 nm laser in addition to the near IR laser for two photon absorption, has afforded control over the degree of polymerisation and reduction evident during fabrication.

Distribution Statement
This is block 12 on the SF298 form.

Distribution A - Approved for Public Release

Explanation for Distribution Statement
If this is not approved for public release, please provide a short explanation. E.g., contains proprietary information.

SF298 Form
Please attach your SF298 form. A blank SF298 can be found here. Please do not password protect or secure the PDF The maximum file size for an SF298 is 50MB.

SF298 14-0048 Wildman.pdf

Upload the Report Document. File must be a PDF. Please do not password protect or secure the PDF . The maximum file size for the Report Document is 50MB.

EOARD report FINAL.pdf

Upload a Report Document, if any. The maximum file size for the Report Document is 50MB.

Archival Publications (published) during reporting period:

Changes in research objectives (if any):

Change in AFOSR Program Manager, if any:

Extensions granted or milestones slipped, if any:

AFOSR LRIR Number

LRIR Title

Reporting Period

Laboratory Task Manager

Program Officer

Research Objectives

Technical Summary

Funding Summary by Cost Category (by FY, $K)

	Starting FY	FY+1	FY+2
Salary			
Equipment/Facilities			
Supplies			
Total			

Report Document

Report Document - Text Analysis

Report Document - Text Analysis

Appendix Documents

2. Thank You

E-mail user

Jan 11, 2016 08:44:12 Success: Email Sent to: matthew.snyder.2@us.af.mil

Response ID: 5656

Survey Submitted:	Jan 11, 2016 8:44 AM
IP Address:	132.3.21.78
Language:	English (en-US)
User Agent:	Mozilla/5.0 (Windows NT 6.1; Win64; x64; Trident/7.0; rv:11.0) like Gecko
Http Referrer:	http://afosr.reports.sgizmo.com/s3/
Page Path:	1 : (SKU: 1) 1 : (SKU: 1) 2 : Thank You (SKU: 2)
SessionID:	1452519389_5693afdd31a7a9.85714258

Response Location

Country:	United States
Region:	AE
City:	Apo
Postal Code:	09464
Long & Lat:	Lat: 0, Long:0